J|A|C|S
ARTICLES
Published on Web 11/23/2002

Tris(trifluoromethyl)borane Carbonyl, $(CF_3)_3BCO$—Synthesis, Physical, Chemical and Spectroscopic Properties, Gas Phase, and Solid State Structure

Maik Finze,[†] Eduard Bernhardt,[†] Annegret Terheiden,[†] Michael Berkei,[†] Helge Willner,*[,†] Dines Christen,[§] Heinz Oberhammer,*[,§] and Friedhelm Aubke[‡]

Contribution from the Fakultät 4, Anorganische Chemie, Gerhard Mercator Universität Duisburg, Lotharstrasse 1, D-47048 Duisburg, Germany, Institut für Physikalische und Theoretische Chemie, Universität Tübingen, 72076 Tübingen, Germany, Department of Chemistry, The University of British Columbia, Vancouver, British Columbia, V6T1Z1, Canada

Received July 19, 2002

Abstract: Tris(trifluoromethyl)borane carbonyl, $(CF_3)_3BCO$, is obtained in high yield by the solvolysis of $K[B(CF_3)_4]$ in concentrated sulfuric acid. The in situ hydrolysis of a single bonded CF_3 group is found to be a simple, unprecedented route to a new borane carbonyl. The related, thermally unstable borane carbonyl, $(C_6F_5)_3BCO$, is synthesized for comparison purposes by the isolation of $(C_6F_5)_3B$ in a matrix of solid CO at 16 K and subsequent evaporation of excess CO at 40 K. The colorless liquid and vapor of $(CF_3)_3BCO$ decomposes slowly at room temperature. In the gas phase $t_{1/2}$ is found to be 45 min. In the presence of a large excess of ^{13}CO, the carbonyl substituent at boron undergoes exchange, which follows a first-order rate law. Its temperature dependence yields an activation energy (E_A) of 112 kJ mol^{-1}. Low-pressure flash thermolysis of $(CF_3)_3BCO$ with subsequent isolation of the products in low-temperature matrixes, indicates a lower thermal stability of the $(CF_3)_3B$ fragment, than is found for $(CF_3)_3BCO$. Toward nucleophiles $(CF_3)_3$-BCO reacts in two different ways: Depending on the nucleophilicity of the reagent and the stability of the adducts formed, nucleophilic substitution of CO or nucleophilic addition to the C atom of the carbonyl group are observed. A number of examples for both reaction types are presented in an overview. The molecular structure of $(CF_3)_3BCO$ in the gas phase is obtained by a combined microwave—electron diffraction analysis and in the solid state by single-crystal X-ray diffraction. The molecule possesses C_3 symmetry, since the three CF_3 groups are rotated off the two possible positions required for C_{3v} symmetry. All bond parameters, determined in the gas phase or in the solid state, are within their standard deviations in fair agreement, except for internuclear distances most noticeably the B—CO bond lengths, which is 1.69(2) Å in the solid state and 1.617(12) Å in the gas phase. A corresponding shift of ν(CO) from 2267 cm^{-1} in the solid state to 2251 cm^{-1} in the gas phase is noted in the vibrational spectra. The structural and vibrational study is supported by DFT calculations, which provide, in addition to the equilibrium structure, confirmation of experimental vibrational wavenumbers, IR-band intensities, atomic charge distribution, the dipole moment, the B—CO bond energy, and energies for the elimination of CF_2 from $(CF_3)_xBF_{3-x}$, $x = 1-3$. In the vibrational analysis 21 of the expected 26 fundamentals are observed experimentally. The ^{11}B-, ^{13}C-, and ^{19}F-NMR data, as well as the structural parameters of $(CF_3)_3BCO$, are compared with those of related compounds.

Introduction

Borane carbonyls can be viewed on account of their high CO stretching wavenumbers as main group analogues of σ-bonded transition metal carbonyl cations.[1,2] In both classes of carbonyls, CO is σ-bonded and the CO bond is polarized by positively charged central atoms, resulting in a strengthening of the CO bond by electrostatic contribution.[3,4] The simplest example of a borane carbonyl, H_3BCO, has been known since 1937.[5] The compound has been extensively characterized by experimental, structural, and theoretical means.[6−9] Approxi-

* To whom correspondence should be addressed. E-mail: willner@uni-duisburg.de. H. Oberhammer: Telephone: 49-7071-295490. Fax: 49-7071-295490. E-mail: heinz.oberhammer@uni-tuebingen.de. F. Aubke: Telephone: 1-604-822-2847. E-mail: aubke@chem.ubc.ca.

[†] Gerhard Mercator Universität Duisburg.

[‡] The University of British Columbia.

[§] Universität Tübingen.

(1) Willner, H.; Aubke, F. *Angew. Chem., Int. Ed. Engl.* **1997**, *36*, 2402−2425.
(2) Willner, H.; Aubke, F. In *Inorg. Chem. Hightlights*; Meyer, G., Naumann, D., Wesemann, L., Eds.; Wiley-VCH: Weinheim Germany, 2002; p 195.
(3) Goldman, A. S.; Krogh-Jespersen, K. *J. Am. Chem. Soc.* **1996**, *118*, 12 159−12 166.
(4) Ehlers, A. W.; Ruiz-Morales, Y.; Baerends, E. J.; Ziegler, T. *Inorg. Chem.* **1997**, *36*, 5031.
(5) Burg, A. B.; Schlesinger, H. I. *J. Am. Chem. Soc.* **1937**, *59*, 780−787.
(6) *Gmelins Handbuch der Anorganischen Chemie, Borverbindungen, Teil 10*; 1980; 1st. Suppl. Volume 1., 1983; 2nd. Suppl. Volume 1, 1987; 3rd. Suppl. Volume 1, 1994; 4th. Suppl. Volume 1a, and 1996, ed.; Volume 1b 1; Springer-Verlag: Berlin, Heidelberg, New York, 1976; Vol. 37.
(7) Venkatachar, A. C.; Taylor, R. C.; Kuczkowski, R. L. *J. Mol. Struct.* **1977**, *38*, 17.
(8) Jones, L. H.; Taylor, R. C.; Paine, R. T. *J. Chem. Phys.* **1979**, *70*, 749.
(9) Bauschlicher, C. W.; Ricca, A. *Chem. Phys. Lett.* **1995**, *237*, 14.

mately twenty additional borane carbonyl derivatives have become known in the meantime. They are synthesized primarily by addition of CO to suitable boranes and boron subhalides.[6]

We have recently reported in a preliminary communication on the synthesis of tris(trifluoromethyl)borane carbonyl, $(CF_3)_3BCO$,[10] by solvolysis of the $[B(CF_3)_4]^-$ anion[11] in concentrated sulfuric acid. This reaction was found accidentaly by testing the limits of stability of the very weak coordinating $[B(CF_3)_4]^-$ anion. The reaction proceeds in a series of ligand transformations, starting from $K[B(CN)_4]$[12] according to (1), featuring a single C-bonded ligand.

$$\left[\text{B}-\text{CN}\right]^- \xrightarrow[-\,0.5\ N_2,\ -\,0.5\ Cl_2]{+\ ClF_3} \left[\text{B}-CF_3\right]^- \xrightarrow[-\,3\ HF]{+\ H_3O^+\,/\,H_2SO_4} \text{B}-\text{CO} \qquad (1)$$

During these transformations, the B−C bonds remain intact, whereas the substituents at the central boron atom are altered first by perfluorination[11] and then by partial hydrolysis.[10] The in situ generation of a B−CO group observed,[10] is unprecedented. The new borane carbonyl is initially identified and characterized by a molecular mass determination, its IR-spectrum (where ν(CO) is unprecedentedly high with 2252 cm^{-1}), NMR-data and a limited number of characteristic reactions.

In this publication, we want to report (i) on details of the synthesis of $(CF_3)_3BCO$ and its thermal behavior, studied by gas phase kinetics, isotopic exchange reactions and low pressure flash thermolysis, with the decomposition products trapped in an Ar-matrix and studied by IR spectroscopy, (ii) the synthesis of the previously unknown reference compound $(C_6F_5)_3BCO$ by trapping the Lewis acid in a CO matrix, (iii) present an overview of a number of chemical reactions, that involve either nucleophilic substitution of the CO ligand or nucleophilic addition to the C atom of the carbonyl group, (iv) the molecular structure of $(CF_3)_3BCO$ in the gas phase, obtained by electron diffraction combined with microwave spectroscopy, (v) the molecular structure of $(CF_3)_3BCO$, obtained by single-crystal X-ray diffraction, (vi) vibrational analysis of $(CF_3)_3BCO$ and DFT calculations, and (vii) a complete characterization of $(CF_3)_3BCO$ by heteronuclear NMR methods.

The comprehensive characterization of $(CF_3)_3BCO$ described here, allows a meaningful and informed comparison to other known carbonyl boranes[5−9] and also to σ-bonded metal carbonyl cations.[1,2]

Experimental Section

General Procedures and Reagents (a) Apparatus. Volatile materials were manipulated in a glass vacuum-line, equipped with two capacity pressure gauges (221 AHS-1000 and 221 AHS-100, MKS Baratron, Burlington, MA) and consisting of three U-traps and valves with PTFE stems (Young, London UK). The vacuum line was connected to an IR cell (Optical path length 200 mm, Si windows, 0.5 mm thick), contained in the sample compartment of a FTIR instrument. Because of this arrangement, it was possible to follow the course of the reactions closely and to monitor the purification processes of the products. Products were stored in flame-sealed glass ampules under liquid nitrogen in a storage Dewar vessel. The ampules were opened and resealed using an ampule key.[13]

The melting point of $(CF_3)_3BCO$ was determined on samples placed inside 6 mm o.d. glass tubes, using a slowly heated stirred water bath, in the temperature range of 5−10 °C. Vapor pressures were measured in a small trap, using the above-mentioned capacitance manometer (AHS-100) in the temperature range between −45 to +10 °C. Five different cold bathes with ethanol as coolant were used to adjust the temperature as quickly as possible to prevent decomposition. Measurements at different temperatures were repeated several times on purified samples to obtain averaged vapor pressure data.

For kinetic measurements, a small glass vessel (1 cm o.d., 10 cm length) equipped with a glass valve with a PTFE stem (Young, London UK) was used. For each run 0.015 mmol $(CF_3)_3BCO$ and 0.8 mmol ^{13}CO were transferred into the evacuated vessel by cooling it to −196 °C. The vessel was placed in a thermostated water bath for the desired time period. The exchange process was quenched by cooling the cell to −196 °C. The excess of ^{13}CO was recovered by cryopumping the gas into a vessel filled with molecular sieve (5 Å) kept at −196 °C. Subsequently, at −78 °C the decomposition products were removed in dynamic vacuum. By warming the vessel to room temperature, the solid residue was finally evaporated into an evacuated IR-cell and the ν(CO) absorbance ratio $A(\nu^{13}_{CO})/A(\nu_{CO})$ was measured. This procedure was performed on 20 samples at bath temperatures of 10.9, 21.0, 25.2, 30.0, and 35.1 °C, respectively. For each temperature, four different reaction times were chosen (between 7 and 300 min).

The potentiometric titration was performed on a 0.1 molar aqueous solution of $(CF_3)_3BCO$ and was repeated several times.

Matrix-isolated samples were prepared by passing a gas stream of Ar, Ne, or N_2 (~3 mmol h^{-1}) over the sample placed in a small U-trap in front of the matrix support. A U-trap containing $(CF_3)_3BCO$ or $(C_6F_5)_3B$ (in this case CO was used as matrix gas) was kept at −82 or +35 °C, respectively. In a stainless steel vacuum line with a volume of 1.1 L, a small amount of a 1:1 CO/BF_3 mixture (ca. 0.1 mmol) was mixed with Ar at a 1:500 ratio. About 1 mmol of this mixture was directly deposited via a stainless steel capillary on the matrix support, kept at 16 K. Details of the matrix apparatus have been described elsewhere.[14]

(b) Chemicals. CO (standard grade, Messer-Griesheim, Krefeld, Germany), ^{13}CO (> 99% isotopic enrichement, Deutero GmbH, Kastellaun, Germany) and $C^{18}O$ (> 99% Ventron, Numbai, India), as well as all standard chemicals and solvents were obtained from commercial sources. H_3BCO was prepared from B_2H_6 and CO as reported.[6] $K[B(CF_3)_4]$ was synthesized as described previously from $K[B(CN)_4]$.[11]

(c) Synthetic Reactions. (1) $(CF_3)_3BCO$. The synthesis was performed in a "V-shaped" reaction vessel, equipped with a valve with a PTFE stem (Young, London) and fitted with two 100 mL round-bottom flasks. Solid $K[B(CF_3)_4]$ (0.5 g/15.3 mmol) was dissolved in 20 mL of Et_2O and transferred into one of the round-bottom flasks, that contained a PTFE-coated magnetic stirring bar. Ether was removed under reduced pressure and 25 mL of concentrated H_2SO_4 were placed into the second round-bottom flask. The reaction vessel was attached to a glass vacuum line with a series of three U-traps and evacuated. H_2SO_4 was added in 3 portions to $K[B(CF_3)_4]$ at room temperature, and the resulting mixture was stirred vigorously. Gas evolution occurred immediately from the suspension. In the 1st U-trap, a liquid, identified as HSO_3F, that had formed during the reaction, was separated at −30 °C. In the 2nd trap $(CF_3)_3BCO$ was collected at −100 °C. Highly volatile byproducts such as BF_3 were solidified at −196 °C in the 3rd U-trap. After completing the addition of H_2SO_4, the reaction mixture was stirred at room temperature until no further gas evolution was observed. The temperature was raised to 45 °C, and the contents of

(10) Terheiden, A.; Bernhardt, E.; Willner, H.; Aubke, F. *Angew. Chem., Int. Ed. Engl.* **2002**, *41*, 799.
(11) Bernhardt, E.; Henkel, G.; Willner, H.; Pawelke, G.; Bürger, H. *Chem.-Eur. J.* **2001**, *7*, 4696.
(12) Bernhardt, E.; Henkel, G.; Willner, H. *Z. Anorg. Allg. Chem.* **2000**, *626*, 560−568.
(13) Gombler, W.; Willner, H. *J. Phys. E: Sci. Instruments* **1987**, *20*, 1286.
(14) Argüello, G. A.; Grothe, H.; Kronberg, M.; Willner, H.; Mack, H. G. *J. Phys. Chem.* **1995**, *99*, 17525.

the flask were stirred for approximately 7 h, until the reaction mixture became clear. 3.31 g of pure $(CF_3)_3BCO$ (13.5 mmol) were obtained from the crude product after trap-to-trap distillation at −85 °C which corresponds to a yield of 88%.

For the syntheses of $(CF_3)_3B^{13}CO$ and $(CF_3)_3BC^{18}O$, a 50 mL round-bottom flask, fitted with a glass valve (Young, London) was charged with 0.24 mmol $(CF_3)_3BCO$ and 5 mmol of ^{13}CO or $C^{18}O$ by vacuum line transfer. The reaction was allowed to proceed at 35 °C 40 min and after subsequent cooling to −196 °C, the excess of isotopically enriched CO was recovered by cryopumping onto molecular sieve (5 Å) at −196 °C. The residue (0.12 mmol) was evaporated and trapped in vacuo at −78 °C. It contained about 50% of $(CF_3)_3B^{13}CO$ or $(CF_3)_3BC^{18}O$, respectively.

(2) $K_2[(CF_3)_3BCO_2]$. A 50 mL round-bottom flask equipped with a valve with a PTFE stem (Young, London), fitted with a PTFE-coated magnetic stirring bar, was charged with 765 mg of $(CF_3)_3BCO$ (3.1 mmol). About 10 mL of distilled water were condensed in vacuo, into the flask, kept at −196 °C. The mixture was allowed to warm to room temperature. Under vigorous stirring, 1.74 g of KOH (31 mmol) dissolved in 5 mL of distilled water was added to the clear colorless solution. After removing most of the water under reduced pressure, the reaction mixture was extracted with CH_3CN three times, in portions of 100, 100, and 50 mL. The collected CH_3CN layers were combined, dried over K_2CO_3 and filtered through a fine glass frit. Even after filtration, the organic solution was cloudy. After removing all volatiles in vacuo, 780 mg (2.30 mmol) 74% yield of white $K_2[(CF_3)_3BCO_2]$ were obtained that showed no impurities in the NMR spectra.

(3) $[Pr_3NH][(CF_3)_3BC(O)OH]$. 780 mg of $K_2[(CF_3)_3BCO_2]$ (2.30 mmol) were dissolved in 20 mL distilled water. Under vigorous stirring, 2 mL (24 mmol) of concentrated HCl and 0.05 mL (5 mmol) of tri-*n*-propyl ammine were added to the clear colorless solution. Immediately after addition small quantities of an off white solid formed and a small amount of the residual ammine was observed on the bottom of the flask. The mixture was extracted with CH_2Cl_2 three times (100 mL, 50 mL and 20 mL, respectively). The collected organic phases were combined, dried over $MgSO_4$ and filtered through a fine glass frit, and the solvent was removed under reduced pressure to yield 794 mg of $[Pr_3NH][(CF_3)_3BC(O)OH]$ (2.12 mmol) 92%. NMR data of the $[Pr_3NH]^+$ cation: ^1H NMR (300.13 MHz, CD_3CN, 25 °C, TMS) δ 9.42 ppm (s, 1 H), 2,96 ppm (t, 6 H), 1,81−1,67 ppm (m, 6H), 0,95 ppm (t, 6H); $^{13}C\{^1H\}$-NMR (125.758 MHz, CD_3CN, 25 °C, TMS) δ 55.12 ppm (s, 1C), δ 17.76 ppm (s, 1C), δ 11.23 ppm (s, 1C).

(4) $(CF_3)_3BNCCD_3$. 130 mg $(CF_3)_3BCO$ (0.5 mmol) were transferred in vacuo into a 5 mm o.d. NMR tube, equipped with a rotational symmetrical valve with a PTFE stem (Young, London).[15] A 1.5-mL portion of dry CD_3CN were condensed to the borane carbonyl and the reaction mixture was warmed to room temperature. Gas evolution was observed in the NMR tube. After 30 min at room temperature, NMR spectra of the mixture were recorded. Nearly pure $(CF_3)_3BNCCD_3$ was identified that contained a small amount (∼4%, ^{19}F NMR) of $(CF_3)_3BC(OH)_2$ as the only impurity.

(d) Preparation of Single-Crystals of $(CF_3)_3BCO$. Approximately 10 mg $(CF_3)_3BCO$ were transferred in vacuo into a small glass ampule (6 mm o.d., 20 cm length) kept at −196 °C. Volatile impurities were removed under reduced pressure at −75 °C and the sealed ampule was stored at −70 °C for 6 d. At this temperature, the vapor pressure of $(CF_3)_3BCO$ was sufficient (10^{-2} mbar) for a slow crystallization process. To prevent decomposition of the single-crystals, used in the subsequent X-ray diffraction analysis, the crystals were placed on a copper trough,[16] cooled to −70 °C. During the preparation the trough was flushed with dry nitrogen. Suitable crystals were selected under a polarizing microscope and fitted into glass capillaries (o.d. 0.1 to 0.3 mm). The capillaries were sealed off at both ends to give glass cylinders of approximately 20 mm length. The glass cylinders, containing the crystals, were attached with wax onto goniometer heads.

Table 1. Crystallographic Data of $(CF_3)_3BCO$ at 143 K

compound	$(CF_3)_3BCO$
empirical formula	C_4BF_9O
formula weight	245.85
crystal system, space group	monoclinic, $P2_1/c$ (No.14)
unit cell dimensions: a [Å]	7.254(1)
b [Å]	9.959(2)
c [Å]	10.793(2)
β [°]	91.18(3)
unit cell volume: V [Å^3]	779.5(2)
Z value	4
ρ_{calc} [g m^{-3}]	2.094
R_1, ($I > 2\sigma(I)$)[a]	0.1271
R_1, (all data)[a]	0.1651
wR_2, (all data)[b]	0.3937

[a] $R_1 = (\sum||F_o| - |F_c||)/\sum|F_o|$. [b] $R_w = [\sum w(F_o^2 - F_c^2)^2/\sum wF_o^2]^{1/2}$, weight scheme $w = [\sigma^2(F_o) + (aP)^2 + bP]^{-1}$, $P = (\max(0, F_o^2) + 2F_c^2)/3$, $a = 0.1823$, $b = 8.1774$.

(e) Instrumentation. (I) Single-Crystal X-ray Diffraction. Diffraction data were collected at −143 K on a Nonius diffractometer with a CCD camera using Mo Kα radiation ($\lambda = 0.710\,69$ Å) and a graphite monochromator. No transformations of the crystal during cooling from −70 to −130 °C were observed optically, but the reflexes became sharper on cooling. At the end of the data collection, the first intensity measurement was repeated, which demonstrated the stability of the crystal during the X-ray diffraction analysis.

The intensity data were subsequently corrected with the SCALEPACK program.[17] The structure was solved in $P2_1/c$ (No. 14) by direct methods with SHELXS-97[18,19] and refined with anisotropic temperature factors.[20] A summary of experimental details and crystal data is collected in Table 1.

(II) Electron Diffraction. Electron diffraction intensities were recorded on Kodak Electron Image plates (13 × 18 cm) with a KD-G2 Diffraktograph[21] at 25 and 50 cm nozzle-to-plate distances and with an accelerating voltage of about 60 kV. The $(CF_3)_3BCO$ sample was kept at −6 °C (sublimation pressure about 10 mbar) and the inlet nozzle was at room temperature. The photographic plates were analyzed by the usual methods[22] and averaged molecular intensities in the s-ranges 2−18 and 8−35 Å^{-1} ($s = (4\pi/\lambda)\sin\theta/2$, λ is the electron wavelength and θ is the scattering angle) are shown in Figure 1.

(III) Microwave Spectroscopy. The microwave spectrum was recorded in the X- and K-bands with a conventional stark spectrometer (modulation frequency 50 kHz). The sample must be allowed to flow continuously through the cell, which was accomplished by cooling the sample to −50 °C, the cell to −30 °C and adjusting the valves accordingly. Broad band as well as high resolution spectra were recorded. Because the broad band spectra were recorded to monitor and ascertain the sample flow through the cell, only the high-resolution spectra were chosen for a subsequent discussion.

(IV) Vibrational Spectroscopy. (a) Gas-phase infrared spectra were recorded with a resolution of 2 cm^{-1} in the range 4000−50 cm^{-1} on a Bruker IFS 66v FTIR instrument. Matrix infrared spectra were recorded using another Bruker IFS 66v FT spectrometer in the reflectance mode employing a transfer optic. A DTGS detector, together with a KBr/Ge beam splitter was used in the region of 5000−400 cm^{-1}. In this region, 64 scans were co-added for each spectrum using an apodized resolution of 1.2 or 0.3 cm^{-1}. A Ge-coated 6 μm Mylar beam splitter and a far-

(15) Gombler, W.; Willner, H. *International Laboratory* **1984**, 84.
(16) Veith, M.; Bäringhausen, H. *Acta Crystallogr., Sect. B: Struct. Sci.* **1974**, *30*, 1806.
(17) Otwinowsky, Z.; Minor, W. *Methods Enzymol.* **1997**, *276*, 307.
(18) Sheldrick, G. M. *Acta Crystallogr., Sect. A: Found. Crystallogr.* **1990**, 467.
(19) Sheldrick, G. M. *SHELXTL, Release 5.1 Software Reference Manual*; Bruker AXS, Inc.: Madison, Wisconsin, USA, 1997.
(20) Sheldrick, G. M. Universität Göttingen, 1997.
(21) Oberhammer, H. *Molecular Structure by Diffraction Methods*; The Chemical Society: London, 1976; Vol. 4.
(22) Oberhammer, H.; Gombler, W.; Willner, H. *J. Mol. Struct.* **1981**, *70*, 273.

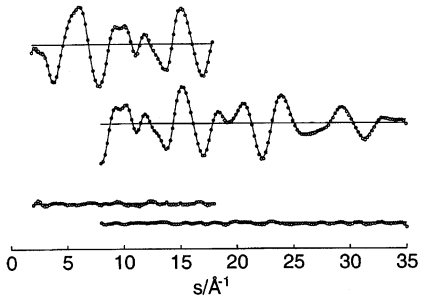

Figure 1. Experimental (dots) and calculated (full line) molecular intensities for long (top) and short (bottom) nozzle-to-plate distances and residuals of $(CF_3)_3BCO$.

IR DTGS detector were used in the region of 650−80 cm^{-1}. In this region, 128 scans were co-added for each spectrum, using an apodized resolution of 0.5 cm^{-1}. (b) Raman spectra of solid $(CF_3)_3BCO$, deposited from the gas phase on a metal finger at −196 °C in high vacuum, were recorded with a resolution of 2 cm^{-1} on a Bruker RFS 100/S FT Raman spectrometer using the 1064 nm excitation (500 mw) of a Nd: YAG laser (DPY 301 II−N−OEM-500, Coherent, Lübeck, Germany).

(V) NMR Spectroscopy. ^{1}H-, ^{19}F-, and ^{11}B-NMR spectra were recorded at room temperature on a Bruker Avance DRX-300 spectrometer operating at 300.13, 282.41 or 96.92 MHz for ^{1}H-, ^{19}F-, and ^{11}B-nuclei, respectively. ^{13}C-NMR spectroscopic studies were performed at room temperature or at −10 °C on a Bruker Avance DRX-500 spectrometer, operating at 125.758 MHz. The NMR signals were referenced against TMS and $CFCl_3$ as internal standards and $BF_3{\cdot}OEt_2$ as external standard. Concentrations of the investigated samples were in the range of 0.1−1 mol L^{-1}. $(CF_3)_3BCO$ samples for NMR spectroscopic studies were prepared in 5 mm NMR tubes, equipped with special valves with PTFE stems (Young, London).[15] Dry SO_2 or CD_2Cl_2 were used as solvents. NMR samples in SO_2 were investigated at −10 °C whereas spectra in CD_2Cl_2 were recorded at room temperature. Salts were dissolved in CD_3CN and transferred into 5 mm o.d. NMR tubes and investigated at room temperature.

(VI) UV Spectroscopy. UV spectra of gaseous samples in a glass cell (optical path length 10 cm) equipped with quartz windows (Suprasil, Heraeus, Hanau, Germany) were recorded on a Perkin−Elmer Lambda 900 spectrometer in the spectral range of 190−350 nm. Pressures were measured with a capacitance manometer (122 A−100, MKS Baratron, Burlington, MA). To eliminate absorption from atmospheric O_2, the monochromator and the housing of the gas cell were flushed with dry N_2.

The uncertainties of IR and UV absorption cross sections (determined on base e) are estimated to be 5 to 10%.

(VII) DSC Measurements. Thermo-analytical measurements were made with a Netzsch DSC204 instrument. Temperature and sensitivity calibrations in the temperature range of 20−500 °C were carried out with naphthalene, benzoic acid, KNO_3, $AgNO_3$, $LiNO_3$, and CsCl. About 5−10 mg of the solid samples were weighed and contained in sealed aluminum crucibles. They were studied in the temperature range of 20−500 °C with a heating rate of 5 K min^{-1}; throughout this process, the furnace was flushed with dry nitrogen. For the evaluation of the output, the Netzsch Protens 4.0 software was employed.

Results and Discussion

Synthetic Aspects and Thermal Properties of $(CF_3)_3BCO$. The synthesis of $(CF_3)_3BCO$ involves the in situ generation of coordinated CO by the solvolysis of a single trifluoromethyl group[10] of the recently reported salt $K[B(CF_3)_4]$[11] in concentrated H_2SO_4 (96%). The formation reaction may be formulated as

$$[B(CF_3)_4]_{(solv)}^- + H_3O^+ \xrightarrow[\text{conc. } H_2SO_4]{25\ ^\circ C} (CF_3)_3BCO_{(g)} + 3HF_{(solv)} \quad (2)$$

The new compound is isolated on account of its volatility. The byproduct HF is converted in H_2SO_4 into HSO_3F, which is detected among the less volatile products of a trap-to-trap condensation.

Precedents for the acid hydrolysis of CF_3 groups which result in the formation of coordinated CO are reported for various complexes of Mn,[23] Fe,[23] Mo,[23] Ru[24], and Pt[25,26] according to eq 3

$$M{-}CF_3 \xrightarrow[HF]{H^+} [M{=}CF_2]^+ \xrightarrow[2HF]{H_2O} [M{-}CO]^+$$

$$M = Mn^{I}, Fe^{II}, Mo^{II}, Ru^{II}, Pt^{II} \quad (3)$$

The reported hydrolysis of CF_3-substituted aryl derivatives in concentrated sulfuric acid under more severe conditions (>100 °C, >6 h) to carboxy derivatives is a more remote precedent.[27] However because in concentrated H_2SO_4, the oxonium ion,[28] H_3O^+, is found to exist, its involvement in the formation of $(CF_3)_3BCO$ (see eq 1) is very likely.

A potential alternate route to $(CF_3)_3BCO$, the CO addition to the Lewis acid $B(CF_3)_3$ is not feasible because the latter compound is so far not known, despite considerable synthetic efforts.[29] In addition, attempts to add CO to the related Lewis acid $B(C_6F_5)_3$,[30,31] which is known since 1963, have been unsuccessful,[32] for reasons which will be discussed below. Hence, the synthesis of $(CF_3)_3BCO$ described here, is both unique and unprecedented.

The new compound $(CF_3)_3BCO$ is a clear, colorless liquid at room temperature, with a melting point of 9 ± 1 °C. At this temperature, the vapor pressure is 38 mbar and the sublimation vapor pressure curve is given by the expression $\ln(p) = -6162/T + 25.5$ (p in mbar, T in K). Above its melting point, $(CF_3)_3BCO$ decomposes rapidly, so that a reliable vapor pressure curve is not obtainable. The thermal decay of $(CF_3)_3BCO$ in the gas phase follows a first-order rate law with $t_{1/2} = 45$ min. The decomposition products CO and BF_3 are identified by IR spectroscopy. Additional IR bands at 1378, 1327, 1244, 1222, 1150, 1130 (sh), 1068, 991, 937, 876, 751, 605 cm^{-1} and new signals in the NMR spectra at $\delta(^{11}B) = +19.4$ and $\delta(^{19}F) = -75.6$, −124.7, and −124.3 ppm indicate the formation of CF_3BF_2 in addition to further, unidentified CF-compounds. Hence, the rate determining step appears to be the dissociation of the B−CO bond. The resulting $B(CF_3)_3$-fragment decomposes fast

(23) Richmond, T. G.; Crespi, A. M.; Shriver, D. F. *Organometallics* **1984**, *3*, 314.
(24) Clark, G. R.; Hoskins, S. V.; Roper, W. R. *J. Organomet. Chem.* **1982**, *234*, C9.
(25) Michelin, R. A.; Facchin, G. *J. Organomet. Chem.* **1985**, *279*, C25.
(26) Appleton, T. G.; Berry, R. D.; Hall, J. R.; Neale, D. W. *J. Organomet. Chem.* **1989**, *364*, 249.
(27) Baasner, B.; Hagemann, H.; Tatlow, J. C.; 4 ed.; Houben-Weyl, 2000; Vol. E10b/Part 2, p 418.
(28) Greenwood, N. N.; Earnshaw, A. *Chemistry of the Elements*; Pergamon Press: Oxford, UK, 1984.
(29) Ansorge, A.; Brauer, D. J.; Bürger, H.; Krumm, B.; Pawelke, G. *J. Organomet. Chem.* **1993**, *446*, 25−35.
(30) Massey, A. G.; Park, A. J.; Stone, F. G. A. *Proc. Chem. Soc.* **1963**, 212.
(31) Massey, A. G.; Park, A. J. *J. Organomet. Chem.* **1964**, *2*, 245.
(32) Jacobsen, H.; Berke, H.; Döring, S.; Kehr, G.; Erker, G.; Fröhlich, R.; Meyer, O. *Organometallics* **1999**, *18*, 1724−1735.

Table 2. IR Bands of Ar Matrix Isolated Products, Formed by Low Pressure Flash Thermolysis of $(CF_3)_3BCO$

band position[a]	I[b]	assignment	band position[a]	I[b]	assignment	band position[a]	I[b]	assignment
2138	0.062	CO	1328	0.090		1102	0.42	CF_2
1510	0.050	$CF_3{}^{10}BF_2$	1230	0.153		984	0.065	
1498	0.017	$^{10}BF_3$	1221	0.196	CF_2	919	0.005	
1458	0.190	$CF_3{}^{11}BF_2$	1211	0.129		755	0.013	
1451	0.025	$^{11}BF_3$	1207	0.178		712	0.004	$CF_3{}^{10}BF_2$
1447	0.079		1180	0.083	C_2F_4	695	0.020	$CF_3{}^{11}BF_2$
1404	0.018		1148	0.085		676	0.003	$^{11}BF_3$
1381	0.015		1143	0.102		605	0.021	
1372	0.067		1135	0.076		559	0.010	
1337	0.023	C_2F_4	1115	0.072		525	0.016	

[a] Most intensive matrix site, cm^{-1}. [b] Absorbance units.

at room temperature, so that the proposed overall decomposition is formulated as shown in eq 4

$$(CF_3)_3BCO \rightleftharpoons CO + (CF_3)_3B \rightarrow CO + CF_3BF_2 + BF_3 + \text{further products} \quad (4)$$

In contrast, BH_3CO is found to decompose in the same IR cell at 28 °C in a different manner. The initial decomposition rate ($t_{1/2} \approx 100$ min), which is comparable to that of $(CF_3)_3BCO$, decreases gradually, as equilibrium (5) is approached

$$2BH_3CO \rightleftharpoons B_2H_6 + 2CO \quad (5)$$

Low pressure flash thermolysis of thermally labile compounds such as $(CF_3)_3BCO$, followed by subsequent quenching of the products in low-temperature matrixes, allows the detection of short-lived intermediates by IR spectroscopy.[14,33] This technique is utilized here, to obtain further information, regarding the first step in the mono-molecular dissociation of $(CF_3)_3BCO$. Initial decomposition products, isolated in an Ar matrix, are observed by passing highly diluted $(CF_3)_3BCO$ and Ar, through a heated spray-on nozzle at 100 °C. At about 180 °C, the initial amount of $(CF_3)_3BCO$ is completely depleted. All matrix IR bands of the decomposition products are simultaneously increased in intensity. The same experiments were repeated by using N_2 as matrix gas in order to form the isoelectronic $(CF_3)_3BN_2$ molecule. However, this attempt failed.

The "new" bands observed in an Ar matrix are listed in Table 2. By comparison to reference matrix IR spectra of authentic samples, the main products CO, BF_3, CF_2, and minor amounts of C_2F_4 are identified. The molar ratio CO/BF_3 of 4:1 is estimated from a reference spectrum of a CO/BF_3 mixture, isolated in an Ar matrix. All additional, unassigned bands in Table 2 can be attributed to a mixture of CF_3BF_2, $(CF_3)_2BF$ and possibly minor amounts of $B(CF_3)_3$. From these observations, the following reaction pathway shown in eq 6 is proposed

$$(CF_3)_3BCO \overset{\text{slow}}{\rightleftharpoons} CO + (CF_3)_3B \quad (6)$$

followed by a series of fast reactions as displayed in eq 7

$$(CF_3)_3B \xrightarrow[-CF_2]{} (CF_3)_2BF \xrightarrow[-CF_2]{} CF_3BF_2 \xrightarrow[-CF_2]{} BF_3 \quad (7)$$

This implies that the activation energy for the CF_2 elimination of $B(CF_3)_3$ is lower, than the B−CO bond energy. Indeed DFT calculations predict for each step in eq 7 values of about 80 kJ mol^{-1}, whereas the B−CO bond energy is estimated to be 114 kJ mol^{-1} (see below).

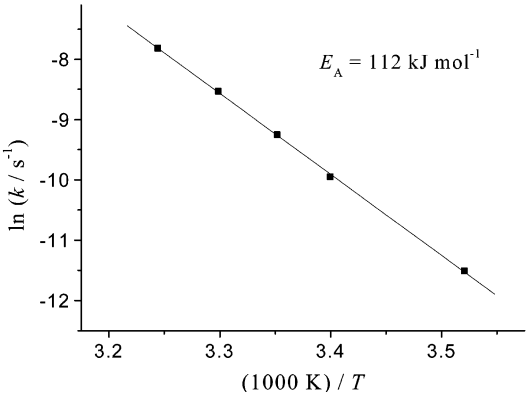

Figure 2. Arrhenius plot of the ^{13}CO exchange reaction with $(CF_3)_3BCO$ (1st order).

The thermal decomposition of $(CF_3)_3BCO$ is in the gas-phase retarded by the presence of CO and in solution by inert aprotic solvents (SO_2, CH_2Cl_2). In the latter case, the solvation of the electrophilic CO carbon atom (see below) by polar solvent molecules, seems to be responsible for a strengthening of the B−CO bond. In the presence of CO the primary step in the decomposition (6) appears to be suppressed, by the backward reaction. The presence of low concentrations of the free Lewis acid $(CF_3)_3B$ in equilibrium with CO is confirmed by the use of isotopically enriched ^{13}CO and $C^{18}O$

$$(CF_3)_3BCO + {}^{13}CO \rightleftharpoons (CF_3)_3B{}^{13}CO + CO \quad (8)$$

which permits the syntheses the ^{13}CO and $C^{18}O$ enriched borane carbonyls.

With ^{13}CO in a large excess, the exchange process (8) is of first order. The exchange rates at 308.3, 303.2, 298.4, 294.2, and 284.1 K are quantitatively determined to be $k = 4.025$, 1.967, 0.9605, 0.4777, and 0.1005×10^{-4} s^{-1}, respectively, by using the observed absorbance ratio $Z = A(\nu^{13}_{CO})/A(\nu_{CO})$ and the equation $\ln(1 + Z) = kt + B$. The corresponding Arrhenius plot of these data is displayed in Figure 2. From the mean square regression slope, $\ln(k) = -13423\ T^{-1} + 35.7$, the activation energy is calculated to be $E_A = 112 \pm 1$ kJ mol^{-1}. This value is in good agreement with the theoretically predicted B−CO bond dissociation energy of 114 kJ mol^{-1} (see below). Hence, the activation energy for the B−CO bond cleavage seems to be nearly identical with the B−CO bond energy. The high value of the frequency factor of 3.2×10^{15} s^{-1} may be due to the high CO pressure of 2.5 bar in kinetic experiments.

(33) Sander, S.; Pernice, H.; Willner, H. *Chem.-Eur. J.* **2000**, *6*, 3645.

Table 3. Thermal and Other Properties of Selected Borane Carbonyl Derivatives[a]

compd	$T_{decomp.}$ [°C][b]	ref	D (B–C) [kJ mol^{-1}]	ref	r(B–C) [Å]	ref	ν_{CO} [cm^{-1}]	ref
F_3BCO	−200	6	7.6	34	2.89	35	2151	36
$(C_6F_5)_3BCO$	−120	[c]	(38)	32	(1.61)	32	2230	[c]
$(CF_3)_3BCO$	0	[c]	112	[c]	1.62	[c]	2252	[c]
H_3BCO	10	[c]	90	[d]	1.53	7	2165	37
$(BF_2)_3BCO$	20	38			1.52	38	2162	39
$(BCl_2)_3BCO$	20	38			1.54	38	2176	38
$1,10-B_{10}H_8(CO)_2$	200	40					2147	40
$1,12-B_{12}H_{10}(CO)_2$	400	40			1.54	41	2210	40

[a] In parentheses: calculated values. [b] Estimated by behavior described in the Literature. [c] This work. [d] Best estimate from five experimental values according to reference.[32]

Scheme 1. Some Selected Chemical Reactions of $(CF_3)_3BCO$

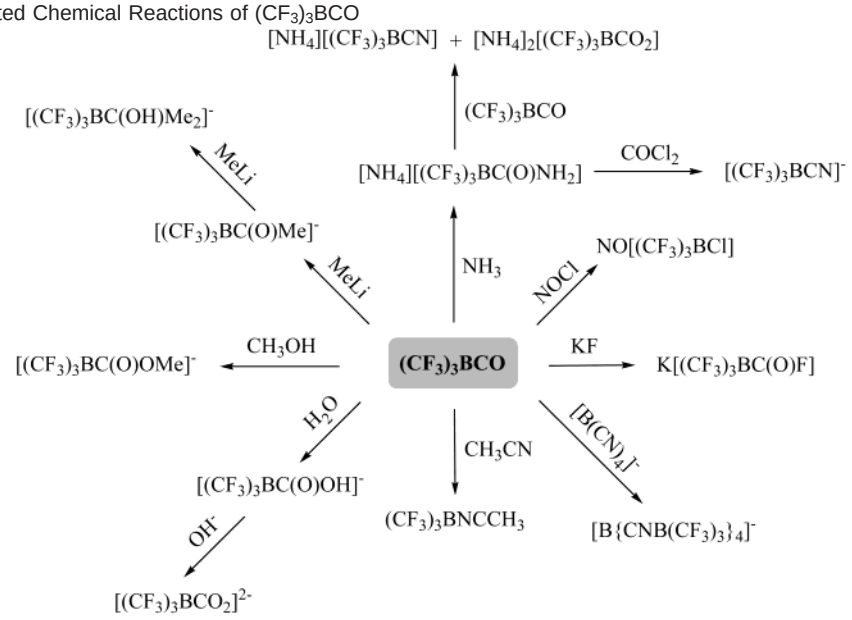

The thermal properties of $(CF_3)_3BCO$ and selected characteristic features are listed in Table 3 and compared to those of other borane carbonyls. In this comparison, the properties of the so far unknown[32] $(C_6F_5)_3BCO$ are of interest. Because any experimental data of this borane carbonyl are unavailable, the compound is synthesized by isolation of $(C_6F_5)_3B$ molecules in solid CO, followed by subsequent slow evaporation of excess CO at 40 K. The solid film of $(C_6F_5)_3BCO$, formed in this manner, exhibits ν(CO) at 2230 cm^{-1} and loses CO at about −120 °C. As can be seen in Table 3, the thermal stabilities of borane carbonyls vary widely and range from −200 °C for F_3-BCO to 400 °C for 1,2-$B_{12}H_{10}(CO)_2$.[11] As far as appropriate data are available, the stabilities seem to correlate well with the D(B−CO) bond energies. The (B−CO) bond lengths for the less stable species are quite large, but in more stable compounds, the (B−CO) bond lengths are invariant and do not appear to reflect the thermal stabilities of the respective species very well. For ν(CO) stretching wavenumbers, which will be discussed later, a simple correlation is not immediately obvious.

The bond-forming reaction between Lewis acids of the type R_3B and Lewis base including CO has recently been analyzed in some detail.[32] It is concluded that the energy required to distort the R_3B unit from its planar ground state to a pyramidal geometry, formed in the R_3B−CO complex, is an important factor. It can hence be argued, that $(CF_3)_3BCO$ should be more stable than $(C_6F_5)_3BCO$. To obtain pyramidal $(C_6F_5)_3B$, required for bonding to CO, more energy is needed than for $(CF_3)_3B$, on account of the bulkier C_6F_5 groups and the possibility, of π-interactions of the aryl π-system with the central boron atom in the trigonally coordinated parent compound. However, the synthetic route to $(CF_3)_3BCO$ by partial hydrolysis of a CF_3 group does not require a change in ground state and the difference between $(CF_3)_3BCO$ and $(C_6F_5)_3BCO$ is reflected in the markedly different thermal stabilities of both compounds. In the *closo*-boranes the pyramidal R_3B fragments are already present and hence very strong B−CO bonds result and carbonyl boranes of unusually high thermal stability.[40]

Chemical Properties of $(CF_3)_3BCO$−An Overview. Reactions of $(CF_3)_3BCO$ with nucleophiles can proceed in two different ways; (i) the attacking nucleophile can react with the carbon atom in an addition to the carbonyl group, which remains bound to the boron atom or (ii) the nucleophile can substitute CO on the central boron atom. Whether nucleophilic addition (i) or substitution (ii) occurs, depends on the relative stability of the resulting products and the nucleophilicities of the attacking reagents. Because, as discussed above, dissociation of $(CF_3)_3BCO$ under reaction conditions is slight, only small amounts of decomposition products are observed and all reactions studied are fairly clean.

As can be seen from an overview of the reactions we have studied so far in Scheme 1, addition reactions to the carbon atom of the CO substituent dominate, where the incoming nucleophile forms stable bonds with carbon. Examples are the reactions with methyllithium, methanol, water, KF, or liquid ammonia. The reactions with CH_3CN and $[B(CN)_4]^-$ result in substitution of the carbonyl by the stronger nucleophile. The

reaction of $(CF_3)_3BCO$ with NOCl also proceeds by exchange of the CO-ligand, giving rise to a novel, convenient synthesis of $[(CF_3)_3BCl]^-$.[42] In reactions, where the CO-ligand is replaced, $(CF_3)_3BCO$ can be viewed as a synthon, used in place of the unknown Lewis acid $(CF_3)_3B$.

Most of the reactions shown in Scheme 1 are fast because of the high reactivity of the borane carbonyl. Hence, the number of byproducts is usually small and in some cases negligible. On account of the highly reactive character of $(CF_3)_3BCO$, the number of solvents, suitable as reaction media, is limited. Especially in SO_2 and CH_2Cl_2, $(CF_3)_3BCO$ is stable and can be stored over a period of one week without any notable decomposition. Unfortunately, reactions with strong bases cannot be performed in these two solvents. In Et_2O, $(CF_3)_3BCO$ is stable at −78 °C for a few hours and reactions with organometallic reagents usually give high yields. THF reacts with $(CF_3)_3BCO$ readily at −78 °C in a ring opening reaction, that gives a complex mixture of anionic esters of the type $[(CF_3)_3BC(O)OR]^-$ and other not identified decomposition products. Ring opening reactions of THF with strong Lewis acids are well-known in the literature.[43]

An interesting reaction is observed between $(CF_3)_3BCO$ and water. Upon dissolving $(CF_3)_3BCO$ in H_2O the dihydroxy carbene complex, $(CF_3)_3BC(OH)_2$, is obtained, according to eq 9

$$(CF_3)_3BCO + H_2O \rightarrow (CF_3)_3BC(OH)_2 \qquad (9)$$

which will undergo ionic dissociation in water (eq 10)

$$(CF_3)_3BC(OH)_2 \underset{+H^+}{\overset{-H^+}{\rightleftharpoons}} [(CF_3)_3BC(O)OH]^- \underset{+H^+}{\overset{-H^+}{\rightleftharpoons}} [(CF_3)_3BCO_2]^{2-} \qquad (10)$$

A potentiometric titration of $(CF_3)_3BCO$ in water reveals pK_a values to be <1.5 and 7.0 for the loss of the first and the second proton, respectively. These values are comparable to those reported for the loss of the first two (4.2) and the second two protons (9.0) of 1,12-$B_{12}H_{10}(CO)_2$ in aqueous solution.[41]

A direct comparison with the pK_a value of isoelectronic $(CF_3)_3CC(O)OH$ is not possible because this compound appears to be unknown. Because $(CF_3)_3CC(O)OH$ should have a smaller pK_a value than trifluoroacetic acid, $CF_3C(O)OH$ (pK_a = 0.23), the comparison of the pK_a value of $CF_3C(O)OH$ with that of $[(CF_3)_3BC(O)OH]^-$ already shows that there is a significant difference. This different behavior is due to the overall negative charge of $[(CF_3)_3BC(O)OH]^-$, that results in an increase of electron density at the carbon atom of the acid. Both anions, $[(CF_3)_3BC(O)OH]^-$ and $[(CF_3)_3BCO_2]^{2-}$, are isolated as stable salts, which are characterized by NMR spectroscopy and their thermal behavior. $[Pr_3NH][(CF_3)_3BC(O)OH]$ is a white solid, that is readily soluble in CH_2Cl_2. It melts at 146 °C and decomposes at 220 °C. In the case of the dianion, the potassium salt $K_2[(CF_3)_3BCO_2]$ is obtained as a white solid, that is insoluble in Et_2O, but soluble in CH_3CN. The salt does not melt before decomposition occurs at 220 °C.

Details on the other reactions and the new compounds, presented in Scheme 1, will be published elsewhere.

Table 4. Rotational Transitions (MHz) in $(CF_3)_3B^{13}CO$ and $(CF_3)_3B^{12}CO$

^{13}C	$J+1 \leftarrow J$	^{12}C
8759.40	7 ← 6	8795.40
18770.63	15 ← 14	18849.00
20021.06	16 ← 15	20102.23
21273.23	17 ← 16	21358.92
22525.20	18 ← 17	22615.60
23777.05	19 ← 18	23870.00
25028.80	20 ← 19	25126.63
26277.18	21 ← 20	26382.82

Molecular Structure of $(CF_3)_3BCO$ in the Gas Phase. (I) Rotational Spectra. Tris(trifluoromethyl)borane carbonyl is a symmetric rotor with a small rotational constant of $B \approx 0.6$ GHz. One therefore expects a spectrum with $J + 1 \leftarrow J$ transitions, approximately 1.2 GHz apart. The structures of the individual transitions depend on centrifugal distortion (K-structure) and nuclear quadrupole coupling. ^{10}B possesses a spin of 3 and a quadrupole moment of 0.086×10^{24} cm^2 approximately (the size of the ^{35}Cl quadrupole moment). ^{11}B with a spin of 3/2 has a quadrupole moment of 0.042×10^{24} cm^2 (intermediate between the quadrupole moments of ^{35}Cl and ^{14}N).

A further complication arises, because the B atom is located in close proximity (~0.2 Å according to ab initio calculations) to the center of mass. As a consequence, the rotational transitions of the ^{10}B- and ^{11}B-isotopomers are still within 1 MHz of one another even at $J = 20$. Hence, it is not possible to resolve any fine- or hyperfine structure by this technique. It is equally impossible to distinguish between the ^{10}B- and ^{11}B-isotopomers. Because the natural abundance ratio of $^{10}B/^{11}B$ is approximately 20:80, we assume in structural calculations, that the observed peaks are due solely to the ^{11}B-isotopomer.

The spectra are mainly recorded in K−Band (18.2−20.1 GHz recorded continuously, narrow ranges recorded in the region of 20.1−26.4 GHz). To check the possibility of resolving the fine structure only, transitions between 8.7 and 10.4 GHz are also recorded under the lowest possible pressure. Even under these conditions, any hyperfine structure remains unresolved. Most of the lines appear as unstructured peaks with a half width of approximately 8 MHz.

With a sample enriched (by approximately 50%) in the ^{13}C-isotopomer, it is possible to measure this isotopomer as well. There are hardly any distinctions between the transitions of the ^{12}C- and ^{13}C-isotopomers in this sample (except for the line positions). The recorded transitions are collected in Table 4 and the resulting rotational constants are found in Table 5. The large half width of rotational transitions results in an accuracy for the rotational constants, that is lower than usual. Thus, the Kraitchman r_s coordinate for the C atom of the CO group, derived from the two B_0 constants (r_s = 1.797(48) Å) possesses a large uncertainty. From the calculated (B3LYP) force field, the vibrational corrections $\Delta B = B_0 - B_z$ are derived. The

(34) Sluyts, E. J.; van der Veken, B. J. *J. Am. Chem. Soc.* **1996**, *118*, 440−445.
(35) Janda, K. C.; Berstein, L. S.; Steed, J. M.; Novick, S. E.; Klemperer, W. *J. Am. Chem. Soc.* **1978**, *100*, 8074−8079.
(36) Gebicki, J.; Liang, J. *J. Mol. Struct.* **1984**, *117*, 283−286.
(37) Bethke, G. W.; Wilson, M. K. *J. Chem. Phys.* **1957**, *26*, 1118−1130.
(38) Jeffery, J. C.; Norman, N. C.; Pardoe, A. J.; Timms, P. L. *Chem. Commun.* **2000**, 2367−2368.
(39) Timms, P. L. *J. Am. Chem. Soc.* **1967**, *89*, 1629.
(40) Knoth, W. H.; Sauer, J. C.; Balthis, J. H.; Miller, H. C.; Muetterties, E. L. *J. Am. Chem. Soc.* **1967**, *89*, 4842−4850.
(41) Fox, M. A.; Howard, J. A. K.; Moloney, J. M.; Wade, K. *Chem. Commun.* **1998**, 2487−2488.
(42) Brauer, D. J.; Bürger, H.; Chebude, Y.; Pawelke, G. *Inorg. Chem.* **1999**, *38*, 3972.
(43) Mair, F. S.; Morris, J. H.; Gaines, D. F.; Owell, D. *J. Chem. Soc., Dalton Trans.* **1993**, 135.

Table 5. Rotational Constants B_0 and B_z of $(CF_3)_3BCO$

	B_0	B_z(exp)	B_z(calcd)[a]
^{12}CO	628.20 (9)	630.14 (29)	629.97
^{13}CO	625.69 (6)	627.63 (29)	627.53

[a] Derived from joint analysis of GED intensities and rotational constants.

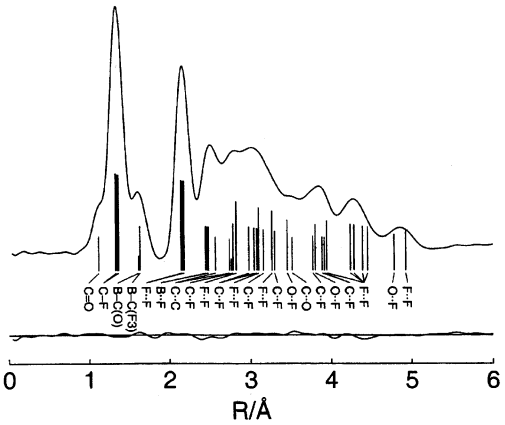

Figure 3. Experimental radial distribution function and difference curve of $(CF_3)_3BCO$.

uncertainty in B_z constants (Table 5) is estimated to be 15% of the correction ΔB. The accuracy of these B_z constants is sufficient for a joint analysis of GED intensities and rotational constants (see below). The r_z coordinate of the C atom of the CO group derived from this analysis (r_z = 1.768(12) Å), reproduces the Kraitchman r_s value within experimental uncertainties.

Gas Electron Diffraction (GED) and Structure Analysis. The radial distribution function (RDF) is calculated by Fourier transformation of the molecular intensities, by applying an artificial damping function $\exp(-\gamma s^2)$ (γ = 0.0019 Å^2). A preliminary structural model which is derived by analysis of the radial distribution function RDF (Figure 3) is refined by least-squares fitting of the molecular intensities. On the basis of quantum chemical calculations, the following assumptions are applied in this refinement: (i) the structure is constrained to C_3 symmetry; (ii) all F−C−F angles in the CF_3 groups are assumed to be equal. According to calculations, these angles deviate by less than 0.5° from the mean value; (iii) the differences between individual C−F bond lengths and the tilt angle of the CF_3 group are set according to the MP2 values; and (iv) vibrational amplitudes, which cause high correlations between geometric parameters or which are poorly determined in the GED experiment, are set equal to calculated (B3LYP/6-31G*) values.

With these assumptions, seven bond parameters, B−CO, B−CF_3, $(C-F)_{avg}$, C−B−C, F−C−F, the dihedral angle ϕ(C−B−C1−F13), and 10 vibrational amplitudes ($l1$ to $l10$) are refined simultaneously. For the B−CO distance, which for this compound is the most interesting parameter, a value of 1.643 Å with a very large uncertainty (3σ value) of ±0.031 Å is obtained.

To derive a more accurate value for the B−CO bond length, a joint analysis of GED intensities and rotational constants is performed. Such an analysis requires the vibrational corrections $\Delta r = r_a - r_z$ for GED parameters and $\Delta B = B_0 - B_z$ for rotational constants. It is well-known, that the concept of perpendicular vibrations results in unrealistically large corrections Δr for bonded distances, if low-frequency−large-amplitude vibrations occur. According to the B3LYP method $(CF_3)_3BCO$ possesses several low-frequency vibrations, such as the CF_3 torsions near 45 cm^{-1} and C−B−C deformations near 90 cm^{-1}.

The concept of perpendicular amplitudes (first harmonic approximation) leads to a correction Δr = 0.025 Å for the C−F bond lengths and such an r_z structure is not compatible with the rotational constants. For this reason, the corrections Δr are calculated with the second harmonic approximation proposed by Sipachev.[44,45] This method results in small corrections for all bond distances (see Table S5). The r_z structure obtained with these corrections, reproduces the experimental rotational constants B_z very well. In the joint least-squares analysis of GED intensities and rotational constants for the parent isotopic species and the ^{13}CO substituted species (CO carbon), the B−O distance is determined very accurately, but the individual B−CO and C−O bond lengths correlate strongly.

Because the primary interest is the B−CO distance, the C−O bond length is fixed. The r_z value for this bond is derived from the r_0 value in CO (r_0 = 1.1308 Å),[46] which is corrected to r_z (1.1321 Å) and then reduced by the calculated (B3LYP) difference between the r_e distance in free CO (1.1379 Å) and that in the complex (1.1298 Å). This leads to r_z = 1.124 Å for the C−O bond length in $(CF_3)_3BCO$. Otherwise, the same assumptions described for the GED analysis are used in the joint analysis. The relative weight of the GED intensities and the rotational constants is adjusted until the B_z values are fitted within their estimated uncertainties (see Table 5). The results of the joint analysis are listed in Table 6 (geometric parameters) and Table S5 (vibrational amplitudes) together with the calculated values. A molecular model is shown in Figure 4.

Molecular Structure in the Solid State. Crystals, suitable for a single X-ray diffraction analysis are grown by sublimation in sealed ampules. Crystallographic data and details on the structure determination are summarized in Table 1. The low quality of the structure is due to a phase transition near −70 °C and the formation of twins. Crystals, which are grown at −20 °C, are disordered and hence not suitable for a single-crystal X-ray structure analysis. When these crystals are cooled below −70 °C, they shatter into pieces. The growth of crystals at temperatures lower than −70 °C is not feasible, because the vapor pressure of $(CF_3)_3BCO$ is too low. Therefore, it is necessary to grow crystals for single-crystal X-ray structure analysis near −70 °C.

A structural analysis of the crystals, grown at −70 °C, confirms at the very least the identity of $(CF_3)_3BCO$ and the correct connectivity of all atoms in the molecule. The bond lengths show uncertainties of about 0.02 Å and their discussion will be limited. The unit cell packing can be described as a molecular lattice, consisting of alternating layers, which are stacked along the *a*-axis. All intermolecular contacts between individual $(CF_3)_3BCO$ molecules in the crystal seem to be longer than the sum of the van der Waals radii.[47,48] The internal bond parameters will be compared below with the gas-phase structure.

Quantum Chemical Calculations. The geometry of $(CF_3)_3$-BCO is optimized with the help of Hatree−Fock and MP2

(44) Sipachev, V. A. *J. Mol. Struct (THEOCHEM)* **1985**, *121*, 143.
(45) Sipachev, V. A. In *Advances in Molecular Structure Research*; Hargittai, I. H., M., Eds.; JAI: Greenwich, 1999; Vol. 5.
(46) Gieliam, O. R.; Johnson, C. M.; Gordy, W. *Phys. Rev.* **1950**, *78*, 140.
(47) Bondi, A. *J. Phys. Chem.* **1964**, *68*, 441.
(48) Alcock, N. W. *Adv. Inorg. Radiochem.* **1972**, *15*, 1.

Table 6. Experimental and Calculated Bond Parameters for $(CF_3)_3BCO$[a]

	$(CF_3)_3BCO_{(g)}$[b]	$(CF_3)_3BCO_{(s)}$	HF/6-311G(2d)	MP2/cc-pVDZ	B3LYP/6-311+G*
		bond length			
C−O	1.124[c]	1.11(2)	1.090	1.138	1.119
B−C	1.617(12)	1.69(2)	1.700	1.610	1.589
B−C1	1.631(4)	1.60(2)	1.626	1.623	1.646
C1−F11	1.358(1)[d]	1.35(2)	1.330	1.366	1.363
C1−F12	1.348(1)[e]	1.35(2)	1.323	1.356	1.355
C1−F13	1.337(1)	1.34(2)	1.314	1.345	1.342
		bond angle			
C−B−C1	103.8(4)	104.4(12)	104.1	105.0	105.5
C1−B−C2	114.5(4)	114.0(12)	114.3	113.5	113.1
F11−C1−F12	107.2(1)	105.7(19)	107.2[g]	107.2[g]	107.3[g]
		torsion angle			
tilt(CF_3)[f]	0.8[c]		0.8	0.9	0.6
τ[h]	11.5(9)	16(3)[i]	15.5	16.1	13.0

[a] Values in Å and °. For atom numbering see Figure 4. [b] r_z values with 2σ uncertainties. [c] Not refined. [d] Difference (C−F2)−(C−F1) set to 0.021 Å. [e] Difference (C1−F12)−(C−F13) set to 0.011 Å. [f] Tilt angle of CF_3 group which makes the B−C1−F12 angle larger than the B−C1−F13 and B−C1−F11 angles. [g] Mean value. [h] Deviation from C_{3v}-symmetry. [i] Average value.

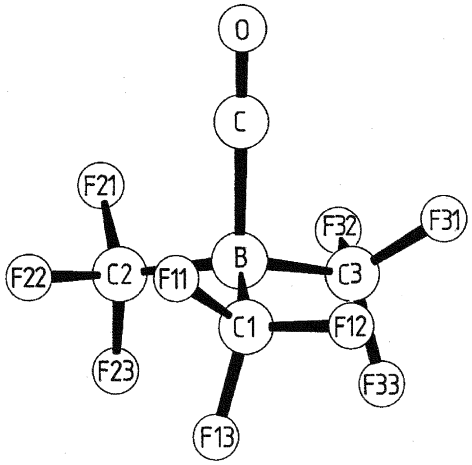

Figure 4. Molecular model and numbering of $(CF_3)_3BCO$.

approximations and with the hybrid method B3LYP, using different basis sets. The vibrational frequencies are calculated with the B3LYP method and 6-31G* basis sets. Vibrational amplitudes and vibrational corrections for interatomic distances and rotational constants are derived from the Cartesian force field (see below). Results for geometric parameters, obtained from calculations with the largest basis sets, vibrational amplitudes, and corrections are listed together with the corresponding experimental values in Table 6 and Table S5.

According to B3LYP/6-31G* calculations, the partial charges q for the atoms within the BCO group are: $q_B = -0.002$, $q_C = +0.404$, and $q_O = -0.166$ e$^-$ respectively. These data support our view, that the C(O) atom is the electrophilic center in $(CF_3)_3$-BCO. In addition a rather high value of 3.27 D is predicted for the dipole moment. Finally the differences in the absolute energies of $(CF_3)_3BCO$, CO, $(CF_3)_xBF_{3-x}$, $x = 1-3$, and CF_2 lead to a B−CO bond energy of 114 kJ mol^{-1} and for the transformation B−CF_3 into B−F + CF_2 to an average energy of 80 kJ mol^{-1}.

All quantum chemical calculations are performed with the GAUSSIAN98 program package.[49]

Discussion of the Gas Phase and Solid State Molecular Structure of $(CF_3)_3BCO$. Tris(trifluoromethyl)borane carbonyl, $(CF_3)_3BCO$, has on account of its convenient physical properties allowed molecular structure determinations in both the gas phase

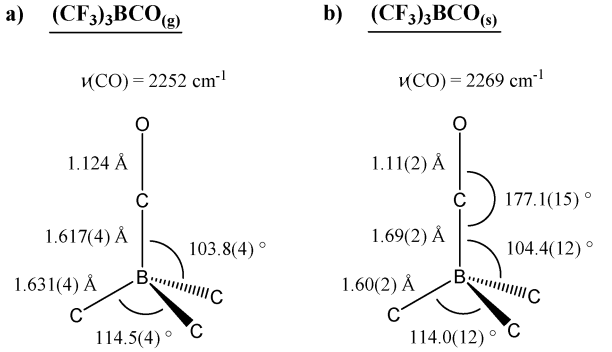

Figure 5. Schematic representation of the molecular structure of $(CF_3)_3$-BCO in the gas phase and in the solid state.

(by electron diffraction and microwave spectroscopy) and the solid state (by single X-ray diffraction). This is to our knowledge unprecedented, for carbonyl boranes and allows a comparison of both sets of structural data for $(CF_3)_3BCO$.

A comparison of internuclear distances (d(B−CF), d(B−CO), and d(C−O)) and selected bond angles for the C_3BCO skeleton of $(CF_3)_3BCO$ is shown in Figure 5. Although the bond angles appear to be identical within stated esd values, the bond lengths show some interesting variations: on going from the gas phase to the solid state, d(B−CF) appears to contract very slightly by about 0.03 Å, just outside the esd limit. More noticeably, the B−CO bond length increases from 1.617(4) Å in the gas phase to 1.69(2) Å in the solid state. Finally, the C−O bond length appears to contract very slightly, best expressed in terms of the CO-stretching wavenumber ν(CO) which increases from 2252 to 2269 cm^{-1} (see Table 7). As a consequence of these changes, all four B−C distances, which are nearly identical in the gas phase, are now in the solid state for d(B−CF) and d(B−CO) different by about 0.09 Å.

(49) Frisch, M. J.; Trucks, G. W.; Schlegel, H. B.; Scuseria, G. E.; Robb, M. A.; Cheeseman, J. R.; Zakrzewski, V. G.; Montgomery, J. A.; Stratmann, R. E.; Burant, J. C.; Dapprich, S.; Millam, J. M.; Daniels, A. D.; Kudin, K. N.; Strain, M. C.; Farkas, O.; Tomasi, J.; Barone, V.; Cossi, M.; Cammi, R.; Mennucci, B.; Pomelli, C.; Adamo, C.; Clifford, S.; Ochterski, J.; Petersson, G. A.; Ayala, P. Y.; Cui, Q.; Morokuma, K.; Malick, D. K.; Rabuck, A. D.; Raghavachari, K.; Foresman, J. B.; Cioslowski, J.; Ortiz, J. V.; Stefanov, B. B.; Liu, G.; Liashenko, A.; Piskorz, P.; Komaromi, I.; Gomperts, R.; Martin, R. L.; Fox, D. J.; Keith, T.; Al-Laham, M. A.; Peng, C. Y.; Nanayakkara, A.; Gonzales, C.; Challacombe, M.; Gill, P. M. W.; Johnson, B.; Chen, W.; Wong, M. W.; Andres, J. L.; Gonzales, C.; Head-Gordon, M.; Replogle, E. S.; Pople, J. A. *Gaussian 98*, Revision A.6; Gaussian, Inc.: Pittsburgh, PA, 1998.

Table 7. Observed and Calculated Band Positions and Band Intensities for the Main Isotopomer[a] of $(CF_3)_3BCO$

		IR				Raman solid −196 °C		assignments according to C_3 symmetry	
cal.[b]	I[c]	gasphase	σ[d]	Ar matrix[e]	I[f]				
		3523	1	3521	0.4			$\nu_1 + \nu_2$	
		2595	1	2604	1.1			$\nu_1 + \nu_9$	
2279	208	2252	156	2251	74	2269	vs	A ν_1	ν(CO)
1278	273	1270	634	1271	154	1270	sh	A ν_2	$\nu_s(CF_3)$
1255	492			1266	230	1266	s	E ν_{14}	$\nu_s(CF_3)$
		1214	40	1218	16			$\nu_5 + \nu_{22}$	
				1196	9			$\nu_6 + \nu_8$	
1197	116	1158	291	1163	261	1173	m	A ν_3	$\nu_{as}(CF_3)$
1189	135			1155	156	1140	w	E ν_{15}	$\nu_{as}(CF_3)$
1157	143	1129	119	1121	141	1119	m	E ν_{16}	$\nu_{as}(CF_3)$
1104	6.5	1074	13	1073	12	1065	w	A ν_4	$\nu_{as}(CF_3)$
930	100	916	221	919	100	891	m	E ν_{17}	$\nu_{as}(BC_3)$
				904	4			$\nu_7 + \nu_9$	
				883	5			$\nu_8 + \nu_9$	
898	3.0	848	10	856	6	867	m	A ν_5	$\nu_s(BC_3)$
722	2.8	725	12	725	5	727	s	A ν_6	$\delta_s(CF_3)$
694	29	698	76	697	29	698	w	E ν_{18}	$\delta_s(CF_3)$
556	4.2	552	4	554	1.8	554	w	E ν_{19}	$\delta_{as}(CF_3)$
516	0.2							A ν_7	$\delta_{as}(CF_3)$
514	0.01	523	6					A ν_8	$\delta_{as}(CF_3)$
513	5.5			523	5.3	525	m	E ν_{20}	$\delta_{as}(CF_3)$
464	12	454	21	453	17	447	m	E ν_{21}	δ(BCO)
366	13	343	7	349	10	357	w	A ν_9	ν(B−CO)
299	1.3	299	3	300	1.5	303	s	E ν_{22}	$\rho(CF_3)$
277	0.3	278	1	278	0.6	283	s	A ν_{10}	$\rho(CF_3)$
254	0.05					260	w	E ν_{23}	$\rho(CF_3)$
246	0.001						A ν_{11}	$\rho(CF_3)$	
122	2.5	132	5	132	2.5	139	w	A ν_{12}	δ(CBC)
117	0.5			125	0.5			E ν_{24}	δ(CBC)
86	0.8	92	2	95	0.5			E ν_{25}	δ(CBC)
41	0.03							E ν_{26}	$\tau(CF_3)$
38	0.01							A ν_{13}	$\tau(CF_3)$

[a] $(^{12}CF_3)_3{}^{11}B^{12}C^{16}O$. [b] B3LYP/6-31G*. [c] Relative band intensity $I(\nu_{17}) \hat{=} 100 = 153$ km mol^{-1}. [d] Absorption cross section 10^{-20} cm^2. [e] Band position at most intensive matrix site. [f] Relative integrated band intensity

Table 8. Comparison of Structural and Spectroscopic Data for $(CF_3)_3BCO$ with Related Compounds and σ-Metal Carbonyl Cations

species	d (X–C) [Å]	d (C–O) [Å]	$\nu(CO)_{avg.}$ [cm^{-1}]	f_{CO} [N m^{-1}]	$\delta(^{13}C)$ [ppm]	ref
CO[a]		1.1281[a]	2143[a]	18.6[a]	184	59−61
$[H-CO]^+$	n.o.[b]	n.o.	2184[a]	21.3[a]	140	62, 63
$[Li-(CO)]^{+c}$	n.o.	n.o.	2185	n.o.	n.o.	64
OBe−CO[d]	n.o.	n.o.	2190	n.o.	n.o.	65
$(CF_3)_3BCO_{(s)}$	1.69(2)	1.11(2)	2269	20.8	159	[e]
$[CH_3-CO]^{+f}$	1.38(2)	1.116(21)	2294	n.o.	150	56, 57, 66
$[N(CO)_2]^{+g}$	1.250	1.118	2340	n.o.	122	58
OCO	1.1615	1.1615	1911	15.5	125	59, 66
$[Fe(CO)_6]^{2+h}$	1.911(5)	1.103(5)	2215	19.7	178	67
$[Os(CO)_6]^{2+h}$	2.027(5)	1.102(7)	2209	19.71	147	2
$[Ir(CO)_6]^{3+i}$	2.029(10)	1.090(10)	2269	20.8	121	68, 69
$[Pt(CO)_4]^{2+h}$	1.982(9)	1.110(9)	2261	20.64	137	70
$[Hg(CO)_2]^{2+h}$	2.083(10)	1.104(12)	2280	21.0	169	71

[a] Gas phase. [b] n.o. = not observed. [c] Li(zeolithe-ZSM-5). [d] Ar-matrix. [e] This work. [f] $[SbF_6]^-$ as counteranion. [g] $[Sb_3F_{16}]^-$ as counteranion. [h] $[Sb_2F_{11}]^-$ as counteranion. [i] In $[Ir(CO)_6][SbF_6]_3 \cdot 4HF$.

This lengthening of the B−CO bond from the gas phase to the solid state observed here, is unusual. Commonly for adducts of boranes with various Lewis acids the opposite trend is observed. For example, the B−N bond in H_3BNH_3 contracts from 1.656(2) Å in the gas phase[50] to 1.564(6) Å in the solid state,[51] which implies tighter, more efficient packing of H_3BNH_3 in the crystal lattice. Other examples are the adducts of acetonitrile and HCN with boron trifluoride.[52,53] The nature of bonding in Lewis acid−base adducts such as H_3BNH_3 or F_3-BNCH has been the subject to several experimental and theoretical studies,[54] and in $(CF_3)_3BCO$ it is clearly different than in the "classical" adducts.

In Table 8 spectroscopic and structural properties of some main group analogues of $(CF_3)_3BCO$ are listed. In the series $(CF_3)_3BCO$, $[CH_3-CO]^+$,[55−57] $[N(CO)_2]^+$,[58] and OCO[59] a

(50) Thorne, L. R.; Suenram, R. D.; Lovas, F. J. *J. Phys. Chem.* **1983**, *78*, 167.
(51) Bühl, M.; Steinke, T.; Schleyer, P. v. R.; Boese, R. *Angew. Chem., Int. Ed. Engl.* **1991**, *30*, 1160.
(52) Dvorak, M. A.; Ford, R. S.; Suenram, R. D.; Lovas, F. J.; Leopold, K. R. *J. Am. Chem. Soc.* **1992**, *114*, 108.
(53) Burns, W. A.; Leopold, K. R. *J. Am. Chem. Soc.* **1993**, *115*, 11 622.
(54) Jonas, V.; Frenking, G.; Reetz, M. T. *J. Am. Chem. Soc.* **1994**, *116*, 8741.
(55) Olah, G. A.; Prakash, G. K. S.; Sommer, J. *Superacids*; Wiley: New York, 1985.
(56) Olah, G. A.; Kuhn, S. J.; Tolgyesi, W. S.; Baker, E. B. *J. Am. Chem. Soc.* **1962**, *84*, 2733.
(57) Boer, F. P. *J. Am. Chem. Soc.* **1966**, *88*, 1572.
(58) Bernhardi, I.; Drews, T.; Seppelt, K. *Angew. Chem.* **1999**, *111*, 2370.

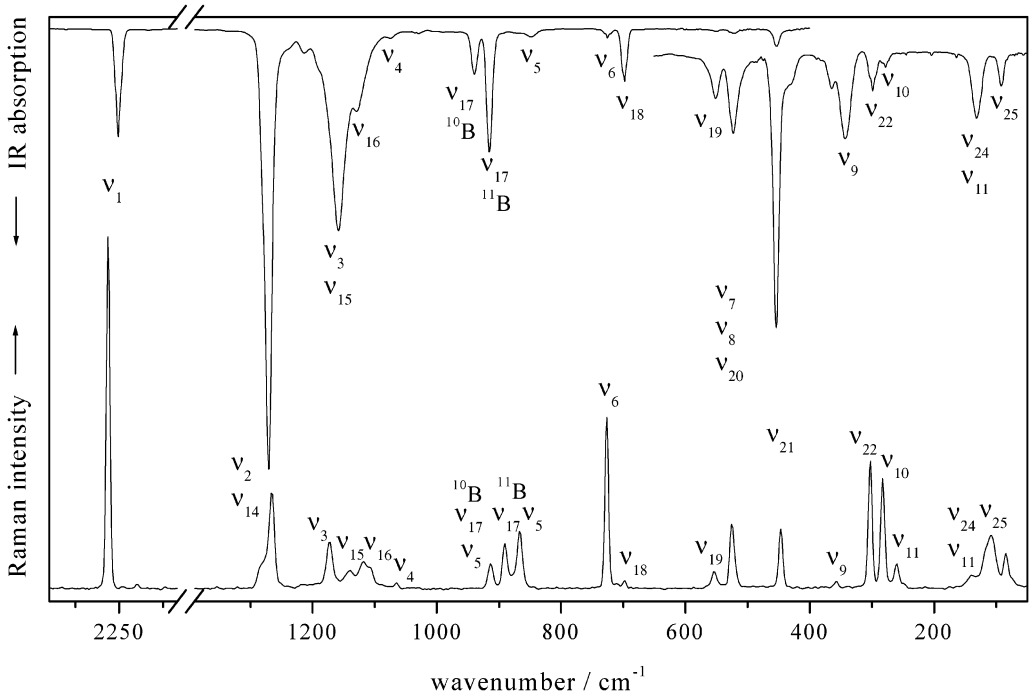

Figure 6. IR (gas phase) and Raman (solid) spectra of $(CF_3)_3BCO$.

decrease of d(X-CO) is observed. The strong similarity between $(CF_3)_3BCO$ and superelectrophilic σ-metal carbonyl cations suggested here, is evident from a comparison of structural and spectroscopic data for solid $(CF_3)_3BCO$ and the homoleptic σ carbonyl cations of the 3d and 5d metals Fe, Hg, Pt, Ir, and Os in Table 8, where f_{CO} and ν(CO) of $(CF_3)_3BCO$ is comparable or occasionally higher than the f_{CO} and $\nu(CO)_{avg}$ values, which are the highest so far observed for metal carbonyl cations.[1,2]

The absence of π-back-bonding is reflected in unusually long M−C bonds.[1,2] This applies also to $(CF_3)_3BCO$. All B−CO bonds of borane carbonyl derivatives of comparable or higher thermal stability than that of $(CF_3)_3BCO$, listed in Table 3, have d(B−CO) values between 1.52 and 1.54 Å. The average B−C distance from the Cambridge listing,[72] based on 29 examples has a value of 1.597 Å and an upper quartile q_u value of 1.611 Å. Even the d(B−CF) values for $(CF_3)_3BCO$ are comparable (in the solid state) or longer (in the gas phase) than the q_u value from the Cambridge index.[72] This is consistent with the absence of π-back-bonding contributions for all C−B bonds. The ease of variation of d(B−CO) in $(CF_3)_3BCO$ by packing effects, indicates a shallow potential curve for this bond in agreement with the low ν(B−CO) vibration of 343 cm^{-1}.

For boranes a strong CH_3/CF_3 substitution effect has been observed. Because $(CF_3)_3B$ is unknown, which precludes a direct comparison with $(CH_3)_3B$, we haven chosen to compare the B−C bonds in $(CH_3)_2BNHMe$ (1.586(2) Å[73]) and in $(CF_3)_2BNMe_2$ (1.623(4) Å[74]). For these two related compounds, a lengthening of the B−C bond on CH_3/CF_3 substitution by about 0.04 Å is observed. The B−CF_3 bond length in the latter compound is very similar to that in $(CF_3)_3BCO$.

As can be seen in Table 6, the results of various quantum chemical calculations, discussed above, are in good agreement with each other, except for the B−CO bond length. This parameter appears to depend on the state of matter and the method of calculation, resulting in a spread from 1.589 Å to ~1.700 Å.

The C−O bond length cannot be determined accurately from experimental data. Quantum chemical calculations predict the C−O internuclear distances in $(CF_3)_3BCO$ to be shorter by 0.008 Å (B3LYP), 0.009 Å (MP2), and 0.013 Å (HF), respectively, than that calculated for free CO.[59] These calculated bond lengths are in agreement with the observed shift in the vibrational frequencies from 2143 cm^{-1} for free CO to 2252 cm^{-1} for $(CF_3)_3BCO$. The respective calculated (B3LYP-MP2, -HF) frequencies are 2208 and 2279 cm^{-1}, respectively.

Vibrational Spectra. The IR and Raman spectra of gaseous and solid $(CF_3)_3BCO$, are shown in Figure 6. Vibrational band positions and intensities are listed in Table 7. They are compared to vibrational data obtained from DFT calculations.

(59) Huber, K. P.; Herzberg, G. *Molecular Spectra and Molecular Structure. Constants of Diatomic Molecules*; van Nostrand: New York, 1979.
(60) Willner, H.; Schaebs, J.; Hwang, G.; Mistry, F.; Jones, R.; Trotter, J.; Aubke, F. *J. Am. Chem. Soc.* **1992**, *114*, 8972.
(61) King, R. B.; Bisnette, M. B. *J. Organomet. Chem.* **1967**, *8*, 287.
(62) de Rege, P. J. F.; Gladysz, J. A.; Horvath, I. T. *Science*; Washington, DC, 1883 **1997**, *276*, 776.
(63) Hirota, E.; Endo, Y. *J. Mol. Spectrosc.* **1988**, *127*, 527.
(64) Katoh, M.; Yamazaki, T.; Ozawa, S. *Bull. Chem. Soc. Jpn.* **1994**, *67*, 7, 1246.
(65) Andrews, L.; Tague, T. J., Jr. *J. Am. Chem. Soc.* **1994**, *116*, 6856.
(66) Kalinowski, H.-O.; Berger, S.; Braun, S. *13C NMR-Spektroskopie*; Georg Thieme Verlag: Stuttgart, 1984.
(67) Bernhardt, E.; Bley, B.; Wartchow, R.; Willner, H.; Bill, E.; Kuhn, P.; Sham, I. H. T.; Bodenbinder, M.; Bröchler, R.; Aubke, F. *J. Am. Chem. Soc.* **1999**, *121*, 7188.
(68) von Ahsen, B.; Berkei, M.; Henkel, G.; Willner, H.; Aubke, F. *J. Am. Chem. Soc.* **2002**, *124*, in press.
(69) Bach, C.; Willner, H.; Wang, C.; Rettig, S. J.; Trotter, J.; Aubke, F. *Angew. Chem., Int. Ed. Engl.* **1996**, *35*, 1974.
(70) Willner, H.; Bodenbinder, M.; Bröchler, R.; Hwang, G.; Rettig, S. J.; Trotter, J.; von Ahsen, B.; Westphal, U.; Jonas, V.; Thiel, W.; Aubke, F. *J. Am. Chem. Soc.* **2001**, *123*, 588−602.
(71) Bodenbinder, M.; Balzer-Jöllenbeck, G.; Willner, H.; Batchelor, R. J.; Einstein, F. W. B.; Wang, C.; Aubke, F. *Inorg. Chem.* **1996**, *35*, 82.
(72) Allen, F. H.; Kennard, O.; Watson, D. G.; Brammer, L.; Orpen, A. G.; Taylor, R. C. *J. Chem. Soc., Perkin Trans. 2* **1987**, S1.
(73) Almenningen, A.; Gundersen, G.; Mangerud, M.; Seip, R. *Acta Chem. Scand., Ser. A* **1981**, *35*, 341.
(74) Hausser, W.; Oberhammer, H.; Bürger, H.; Pawelke, G. *J. Chem. Soc., Dalton Trans.* **1987**, 1839.

$(CF_3)_3BCO$ possesses C_3 symmetry and the irreducible representations of fundamental vibrations and their activities are in accordance to eq 11

$$\Gamma_{vib} = 13A\ (IR, Ra\ p) + 13\ E\ (IR, Ra\ dp) \qquad (11)$$

for a total of 26 IR and Raman active vibrational fundamentals. Of these possible 26 fundamentals of $(CF_3)_3BCO$, the wavenumbers of 21 fundamentals are obtained experimentally. The "missing" CF_3 torsional modes ν_{13} and ν_{26} are expected at ~38 and 41 cm^{-1} and judged to be outside the range of our spectrometer. The other missing bands are, according to calculations, too weak for detection. Also in the IR gas-phase spectrum, the bands due to several fundamentals overlap which each other. To achieve resolution, IR matrix data are included in Table 7. Because the most intensive band at 1266 cm^{-1} (ν_{14}) is not completely resolved, even in Ar matrix, the single strong band at 919 cm^{-1} (ν_{17}) is chosen as reference for relative intensity determinations.

As can be seen in Table 7, the agreement between experimental and calculated band positions and IR band intensities is reasonable. This allows an assignment of all 26 fundamentals. In addition, the assignments are supported by experimental and calculated isotopic shifts listed in Table S6. Isotopic shifts are obtained from IR measurements on $(CF_3)_3B^{13}CO$ and $(CF_3)_3BC^{18}O$ isotopically enriched molecules, isolated in Ne, Ar, and N_2 matrixes.

The three different matrix materials allow us to distinguish between matrix and isotopic splitting. The average isotopic shifts of the three matrix spectra are listed in Table S6. The assignments of all bands are unambiguous, except for that of ν_5. This fundamental is expected to appear near 900 cm^{-1} with a ^{10}B satellite at 935 cm^{-1}. However, three bands of similar intensity are observed in this region. This is only possible if one or two combination modes are in anharmonic resonance with ν_5. The fundamental should be the most intensive band (found at 856 cm^{-1}, Ar-matrix). Because the change of this band pattern is stronger on $C^{18}O$ substitution as on ^{13}CO substitution, we assume the resonance partners to be ($\nu_7 + \nu_9$) and ($\nu_8 + \nu_9$).

The approximate description of modes, presented in Table 7, is based on the calculated displacement vectors of the atoms in the respective modes and the observed isotopic shifts. Very characteristic is the ν(CO) stretching vibration at 2252 cm^{-1} (gas phase). This mode is found in the solid state with 2269 cm^{-1} at an even higher wavenumber and correlates well with the longer B−CO bond in solid $(CF_3)_3BCO$ as discussed.

Hence, $(CF_3)_3BCO$ has among borane carbonyls (see Table 3) the highest CO stretching wavenumber reported so far. Isotopic shifts for $^{12/13}CO$ (52.3 cm^{-1}) and $C^{16/18}O$ (50.5 cm^{-1}) differ slightly from calculated values, based on the two mass model (50.1, 54.3 cm^{-1} respectively). This could be an indication of some slight vibrational mixing.

A characteristic feature of all borane carbonyls, is the observation of the CO stretch at higher wavenumbers than for gaseous CO (2143 cm^{-1}). This is mainly due to a bond polarization of the CO ligand attached to boron.[3,4] The positive charge on the carbon atom of CO in the borane carbonyl is the result of (i) the high electron affinity or Lewis acidity of the R_3B fragment, (ii) the length of the (B−CO) bond, (iii) the electropositive nature of boron within the $B(R_3)_3$ group, and (iv) the lack of π(B → CO) back-bonding.

In $(CF_3)_3BCO$ the electron affinity of the Lewis acidic fragment, $B(CF_3)_3$, is expected to be high. The B−CO bond length of 1.69(2) Å indicates the proposed CO bond polarization and the charge of the B atom is increased, due to the high electronegativity of the CF_3 groups. Furthermore, there should be very little π-back-bonding in the case of CF_3 ligands. These combined contributions explain the extremely high ν(CO) value of $(CF_3)_3BCO$.

The six C−F stretching vibrations of the symmetry type 3A + 3E are observed in the expected range of 1074−1271 cm^{-1}. Of these, the in phase $\nu_s(CF_3)$ stretch, ν_2, exhibits the highest wavenumber and shows an $^{10/11}B$ isotopic shift of 2.5 cm^{-1}, due to some vibrational mixing with $\nu_s(BC_3) = \nu_5$. The out of phase ν_s CF_3-stretch, ν_{14}, appears to be slightly lower in energy. The large $^{10/11}B$ isotopic shift of 14.5 cm^{-1} is due to strong vibrational mixing with $\nu_{as}(BC_3) = \nu_{17}$.

All remaining CF_3-vibrations are fairly isolated. They are in order of decreasing wavenumbers followed by the two $\nu(BC_3)$ vibrations ν_{17} and ν_5 at 931 and 880 cm^{-1} respectively. The $\delta(CF_3)$ deformation modes are observed in the region of 730−510 cm^{-1} and are assigned according to the calculated symmetry type and the atom displacement vectors. The next two vibrations at lower wavenumbers of 454 and 343 cm^{-1} are sensitive toward isotopic substitution of the CO group and are best described as δ(BCO) and ν(B−CO), respectively. The latter vibration is coupled weakly with ν(CO). All low frequency skeletal vibrations are extensively mixed and a description of these modes is somewhat arbitrary.

UV Spectrum. The UV spectrum of $(CF_3)_3BCO$ features according to Figure S1 in the Supporting Information a single high energy electronic transition with a maximum <190 nm (outside the range of our instrument) and an onset at about 220 nm. This is consistent with the noted lack of color for $(CF_3)_3BCO$.

NMR Spectra. Tris(trifluoromethyl)borane carbonyl, $(CF_3)_3BCO$, its reaction products with water, the anions $[(CF_3)_3BC(O)OH]^-$ and $[(CF_3)_3BCO_2]^{2-}$, and the adduct $(CF_3)_3BNCCD_3$, are subject of detailed ^{11}B- and ^{19}F-NMR spectroscopic investigations. $(CF_3)_3BCO$, $[(CF_3)_3BC(O)OH]^-$, and $(CF_3)_3BNCCD_3$ are also investigated by ^{13}C-NMR. Furthermore $(CF_3)_3BC(OH)_2$ is observed as an impurity in the mixture of the reaction of $(CF_3)_3BCO$ with CD_3CN. A spectroscopic characterization by ^1H-, ^{11}B-, and ^{19}F-NMR will be given of all compounds mentioned above. All relevant data are listed in Table 9. The ^{19}F-NMR spectra of the borane carbonyl, $[(CF_3)_3BC(O)OH]^-$, and $[(CF_3)_3BCO_2]^{2-}$ are shown in Figure 7 and the ^{11}B-NMR spectra are displayed in Figure 8. Furthermore the ^{13}C-NMR spectra of $(CF_3)_3BCO$ and $[(CF_3)_3BC(O)OH]^-$ are shown in Figures 9 and 10, respectively.

In the ^{11}B- and ^{19}F-NMR spectra, the compounds show signals in the typical range of tetrahedrally coordinated boron species, with three CF_3 groups attached to boron.[11,77] In the ^{19}F-NMR spectra the signal of each compound is split into a quartet, due to coupling with the ^{11}B-nucleus. Furthermore for $[(CF_3)_3BC(O)OH]^-$, $[(CF_3)_3BCO_2]^{2-}$, and $(CF_3)_3BC(OH)_2$ ^{10}B satellites

(75) Brauer, D. J.; Bürger, H.; Chebude, Y.; Pawelke, G. *Eur. J. Inorg. Chem.* **1999**, *2*, 247.
(76) Brauer, D. J.; Pawelke, G. *J. Organomet. Chem.* **2000**, *604*, 43.
(77) Pawelke, G.; Bürger, H. *Coord. Chem. Rev.* **2001**, *215*, 243.

Table 9. NMR-Data of $(CF_3)_3BCO$ and Related Species[a]

compd	$\delta(^{11}B)$ [ppm]	$\delta(^{13}C)$ CF_3 [ppm]	$\delta(^{13}C)$ [ppm]	$\delta(^{19}F)$ [ppm]	$^1J(^{11}B,^{13}C)$ CF_3 [Hz]	$^1J(^{11}B,^{13}C)$ [Hz]	$^1J(^{13}C,^{19}F)$ [Hz]	$^2J(^{11}B,^{19}F)$ [Hz]	$^3J(^{13}C,^{19}F)$ CF_3 [Hz]	$^3J(^{13}C,^{19}F)$ [Hz]	$^4J(^{19}F,^{19}F)$ [Hz]	ref
$(CF_3)_3BCO$, CD_2Cl_2	−17.9	126.2	159.8	−58.7	80 ± 5	30 ± 5	298 ± 3	36 ± 2	n.o.[b]	n.o.	n.o.	c
$(CF_3)_3BCO$, SO_2	−17,8	126.7	158.9	−58.3	75 ± 10	30 ± 10	298 ± 3	32 ± 2	n.o.	n.o.	n.o.	c
$[(CF_3)_3B(OH)]^-$	−10.6	134.7		−68.0	75.8		311.4	26.8	2.7		n.o.	75
$(CF_3)_3BC(OH)_2$[d]	−18.7	n.o.	n.o.	−60.3	n.o.	n.o.	n.o.	27.2	n.o.	n.o.	n.o.	c
$[(CF_3)_3BCO_2]^{2-}$	−19.1	n.o.	n.o.	−60.3	n.o.	n.o.	n.o.	25.8	n.o.	n.o.	n.o.	c
$[(CF_3)_3BC(O)OH]^-$	−18.9	133.9	186.4	−60.4	72.8	68.2	305.5	25.8	4.0	3.5	n.o.	c
$[(CF_3)_3BC(O)OD]^-$, D_2O	−19.0	135.0	192.5	−60.6	72.8	67.0	305.1	25.8	4.0	3.4	6.3	c
$(CF_3)_2BNMe_3(C(O)OH)$	−10.8	132.2	184.4	−60.3	77.1	73.7	305.0	28.0	n.o.	n.o.	n.o.	76
$[B(CF_3)_4]^-$	−18.9	132.9		−61.6	73.4		304.3	25.9	3.9		5.8	11
$[(CF_3)_3BCN]^-$	−22.3	132.5	127.5	−62.1	75.9	64.0	304.3	29.0	n.o.	n.o.	n.o.	11
$(CF_3)_3BNCCD_3$[e]	−15.1	129.4		−65.9	n.o.		∼296	∼24	n.o.		n.o.	29 c

[a] NMR-solvent if not specified otherwise: CD_3CN. [b] n.o. = not observed. [c] This work. [d] ^1H NMR: $\delta(OH) = 11.06$ ppm. [e] ^1H NMR: $\delta(CD_2H) = 2.79$ ppm, $^2J(^1H,^2D) = 2.06$ Hz, ^{13}C NMR: $\delta(CD_3) = 5.0$ ppm, $^1J(^2D,^{13}C) = 21.6$ Hz, $\delta(NC) = 122.1$ ppm.

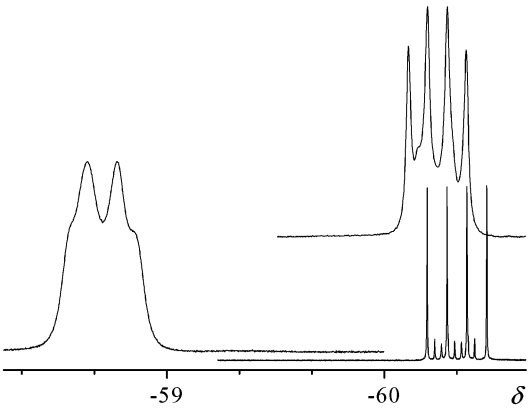

Figure 7. ^{19}F NMR spectra of $(CF_3)_3BCO$ (left), $[(CF_3)_3BC(O)OH]^-$ (right) and $[(CF_3)_3BCO_2]^{2-}$ (top).

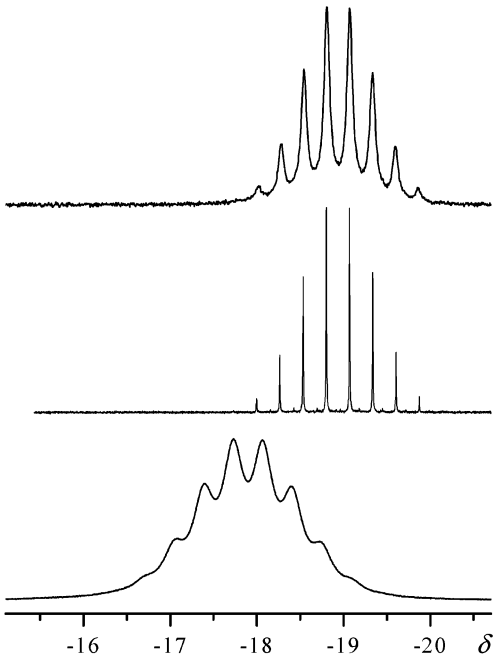

Figure 8. ^{11}B NMR spectra of $(CF_3)_3BCO$ (bottom), $[(CF_3)_3BC(O)OH]^-$ (middle) and $[(CF_3)_3BCO_2]^{2-}$ (top).

are observed as septets, with intensities according to the relative abundances of the nuclei.

The ^{11}B-NMR signals are split into decets because of the coupling with nine equivalent ^{19}F-nuclei. In both ^{11}B- and ^{19}F-NMR spectra, the signals of $[(CF_3)_3BC(O)OH]^-$, $[(CF_3)_3BCO_2]^{2-}$, and $(CF_3)_3BC(OH)_2$ are shifted to lower frequencies, compared to the signals of $(CF_3)_3BCO$. The ^{11}B- and ^{19}F-NMR shifts of the substances, obtained from the reaction with water, are very similar and it is not possible, to assign the observed signals to a specific species, by comparison of the chemical shifts alone.

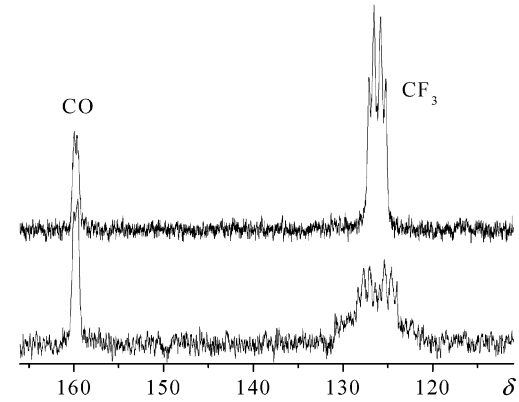

Figure 9. ^{13}C NMR spectrum (bottom) and $^{13}C\{^{19}F\}$ NMR spectrum (top) of $(CF_3)_3BCO$.

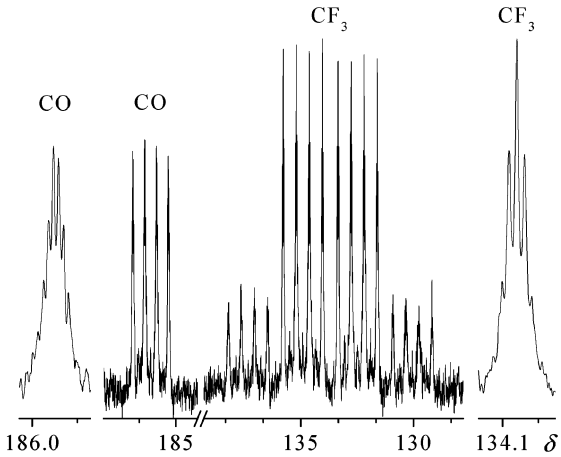

Figure 10. ^{13}C NMR spectrum of $[(CF_3)_3BC(O)OH]^-$. The expanded sections of the two signals show the $^3J(^{13}C,^{19}F)$ coupling patterns.

In Figures 9 and 10, the ^{13}C-NMR spectra of $(CF_3)_3BCO$ and $[(CF_3)_3BC(O)OH]^-$ are shown, respectively. In both ^{13}C-NMR spectra, the signal and the $^1J(^{13}C,^{19}F)$ coupling of the C atoms of the CF_3 groups is in the typical range of CF_3 groups attached to boron (Table 9). The CO carbon atom of $(CF_3)_3BCO$ shows a signal at 159 ppm, which is in the range of transition metal carbonyl cations[1] and other related species (Table 8).

Table 10. Relaxation Times of $(CF_3)_3BCO$ and Related Species

compd	T_1[a] [ms]	σ_1[b] [Hz]	T_2[c] [ms]	σ[d] [Hz]	σ_1/σ	$\Delta(\sigma)$[e] [Hz]
$(CF_3)_3BNCCD_3$	6	53	5−6	50−70	1−0.8	0−17
$(CF_3)_3BCO$	10	32	11−5	30−60	1−0.5	0−28
$[(CF_3)_3BCO_2]^{2-}$	52	6	40	8	0.8	2
$(CF_3)_3BC(OH)_2$	157	2	80−106	3−4	0.7−0.5	1−2
$[(CF_3)_3BCN]^-$	181	1.8	144	2.2	0.8	0.4
$[(CF_3)_3BC(O)OH]^-$	746	0.43	490	0.65	0.7	0.22
$[B(CF_3)_4]^-$	39358	0.008	3183	0.10	0.08	0.09

[a] $I_\tau = I_0 + p\cdot\exp(-\tau\cdot T_1)$. [b] $\sigma_1 = (\pi\cdot T_1)^{-1}$. [c] $T_2 = (\pi\cdot\sigma)^{-1}$. [d] Measured line width. [e] $\sigma - \sigma_1$.

The carbon atom of the acid function in $[(CF_3)_3BC(O)OH]^-$ has a chemical shift of 186 ppm which is typical for the carbon atoms of carboxylic acids.[66] For both species, the signals of the CF_3 groups as well as the signals of the CO ligand or of the C(O)OH ligand are split into quartets, due to coupling with ^{11}B. In the case of $[(CF_3)_3BC(O)OH]^-$, the ^{10}B satellites are shown and furthermore the $^3J(^{13}C,^{19}F)$ couplings are resolved. In the ^{13}C-NMR spectra of $(CF_3)_3BNCCD_3$, the signals of the carbon atoms of the coordinated d^3-acetonitrile are shifted to higher frequencies, relative to free d^3-acetonitrile. The signal due to the CF_3 groups is in the same range, as the signals of the compounds described above.

In the ^1H-NMR spectrum of $(CF_3)_3BC(OH)_2$, the signal of the hydroxy protons are observed with a chemical shift of $\delta =$ 11.1 ppm, which is typical for acidic protons.[78] In the case of $[(CF_3)_3BC(O)OH]^-$, it is not possible to measure the signal of the acidic proton, probably due to a fast exchange process.

$(CF_3)_3BCO$ and $(CF_3)_3BNCCD_3$ show very broad signals (Table 10). This behavior is a typical feature of $^{11}B-NMR$ due to the quadrupolar moment of the ^{11}B-nucleus.[79,80] In Table 10, the T_1 values of ^{11}B of some compounds described herein are listed. The values are compared to the T_2 values, calculated from the measured line width. For substances with a line width greater than 0.5−1.0 Hz in the ^{11}B-NMR spectra, the relaxation time is determined by the quadrupolar relaxation. The ^{19}F-NMR signals of the carbonyl and the acetonitrile adduct are broadened as well, because of the coupling with the ^{11}B-nucleus.

In the ^{13}C- and ^{19}F-NMR spectra of $(CF_3)_3BCO$ (Figures 7 and 9) and $(CF_3)_3BNCCD_3$ the NMR signals are distorted and the usual quartet with four signals of equal intensity is not found. It is well-known that the spectrum of a nucleus A coupled to another nucleus B with a spin >1/2 differs from the expected multiplet structure if the inverse spin−lattice relaxation rate σ_1 of nucleus B is comparable to the coupling constant $J(A,B)$.[80−82] By comparison of the σ_1 values (Table 10) with the coupling constants $^1J(^{13}C,^{11}B)$ and $^2J(^{19}F,^{11}B)$ (Table 9) it can be understood why the distortion is observed in the cases of $(CF_3)_3$-BCO and $(CF_3)_3BNCCD_3$ and not in the case of $[(CF_3)_3$-$BC(O)OH]^-$. Especially the comparison of the line shapes of the two ^{13}C-NMR signals of $(CF_3)_3BCO$ rationalizes this observation, since the signal of the CO ligand with the smaller $^1J(^{13}C,^{11}B)$ is much more distorted, than the signal of the CF_3 groups which shows the larger coupling constant $^1J(^{13}C,^{11}B)$.

The ^{19}F-NMR spectrum of $[(CF_3)_3BCO_2]^{2-}$ shows the beginning of a distortion. In the $^{11}B-NMR$ spectra of the compounds, a similar distortion effect is not observed and the usual intensity distribution as well as the true $^2J(^{19}F,^{11}B)$ value is found. Hence, it can be excluded that exchange of the CO ligand is responsible for the line broadening and distortion of the signal pattern.

Summary and Conclusion

Tris(trifluoromethyl)borane carbonyl, $(CF_3)_3BCO$, which is formed in a unique, unprecedented reaction, the partial hydrolysis of a single CF_3 group of the anion $[B(CF_3)_4]^-$[11] in concentrated H_2SO_4,[10] has been extensively characterized. Its thermal stability has been explored and a decomposition pathway is established. A first glance of its potential as chemical reagent has been obtained. Its molecular structure has been determined by a combination of electron diffraction and microwave spectroscopy in the gas phase and by single-crystal X-ray diffraction. Its rotational and vibrational spectra are reported. Vibrational assignments are made with the help of ^{13}C and ^{18}O isotopomers and supported by density functional theory (DFT) calculations. The characterization of $(CF_3)_3BCO$ is completed by ^{11}B, ^{13}C and ^{19}F NMR spectroscopy.

Like the synthetic route, the spectroscopic and structural properties are unique among borane carbonyls. The structural features, $d(B-C)$ and $d(C-O)$, and the spectroscopic features $\nu(CO)$, f_{CO} and $\delta(^{13}C)$ are compared to those of related main group species and the superelectrophilic σ-metal carbonyl cations: linear $[Hg(CO)_2]^{2+}$,[71] square planar $[Pt(CO)_4]^{2+}$,[70] octahedral $[Fe(CO)_6]^{2+}$,[67] $[Os(CO)_6]^{2+}$ [2] and $[Ir(CO)_6]^{3+}$.[68,69] This comparison reveals a remarkable similarity because in all instances the bond between CO and E, E = B, Hg^{2+}, Pt^{2+} and Ir^{3+}, is a pure σ-bond and the C atom(s) of the CO ligand(s) is (are) the electropositive center(s).

Acknowledgment. Financial support by the Deutsche Forschungsgemeinschaft, DFG, and the Fonds der Chemischen Industrie is acknowledged. Furthermore, we are grateful to Merck KGaA, Darmstadt, Germany, for providing financial support and chemicals used in these studies. We thank Professor Frohn for a sample of $B(C_6F_5)_3$, Mr. M. Zähres for performing some NMR measurements, and Dr. Ljudmilla V. Kristenko, University of Moscow, for calculating vibrational amplitudes and corrections with the program of Sipachev. Professor Minkwitz, University of Dortmund, is gratefully acknowledged for allowing the use of the CCD diffractometer.

Supporting Information Available: A complete table of crystallographic data, a table of atomic coordinates in the crystal structure, a table of selected bond length and angles in the crystal structure, a table of the anisotropic displacement factors, a table of interatomic distances, experimental (GED) and calculated vibrational amplitudes and vibrational corrections, a table of the observed and calculated isotopic shifts of the fundamental vibrations of $(CF_3)_3BCO$, the UV spectrum, a view of the molecule in the crystal structure and a view of the unit cell. This material is free of charge via the Internet at http://pubs.acs.org. Details of the crystal structure determination can be obtained from the Fachinformationzentrum Karlsruhe, D-76344 Eggenstein-Leopoldshafen, Germany, (Fax: 49−7247−808−666; E-mail: crysdata@fiz.karlsruhe.de) on quoting the depository number CSD-412578.

JA0209924

(78) Hesse, M.; Meier, H.; Zeeh, B. *Spektroskopische Methoden in der organischen Chemie*, 4 ed.; Georg Thieme Verlag: Stuttgart, 1991.
(79) Hubbard, P. S. *J. Chem. Phys.* **1970**, *53*, 985.
(80) Halstead, T. K.; Osment, P. A.; Sanctuary, B. C.; Tagenfeldt, J.; Lowe, I. J. *J. Magn. Reson.* **1986**, *67*, 267.
(81) Abragam, A. *Principles of Nuclear Magnetism*; Clarendon Press: Oxford, 1986.
(82) Bendel, P. *J. Magn. Reson.* **1995**, *Ser. A 117*, 143.